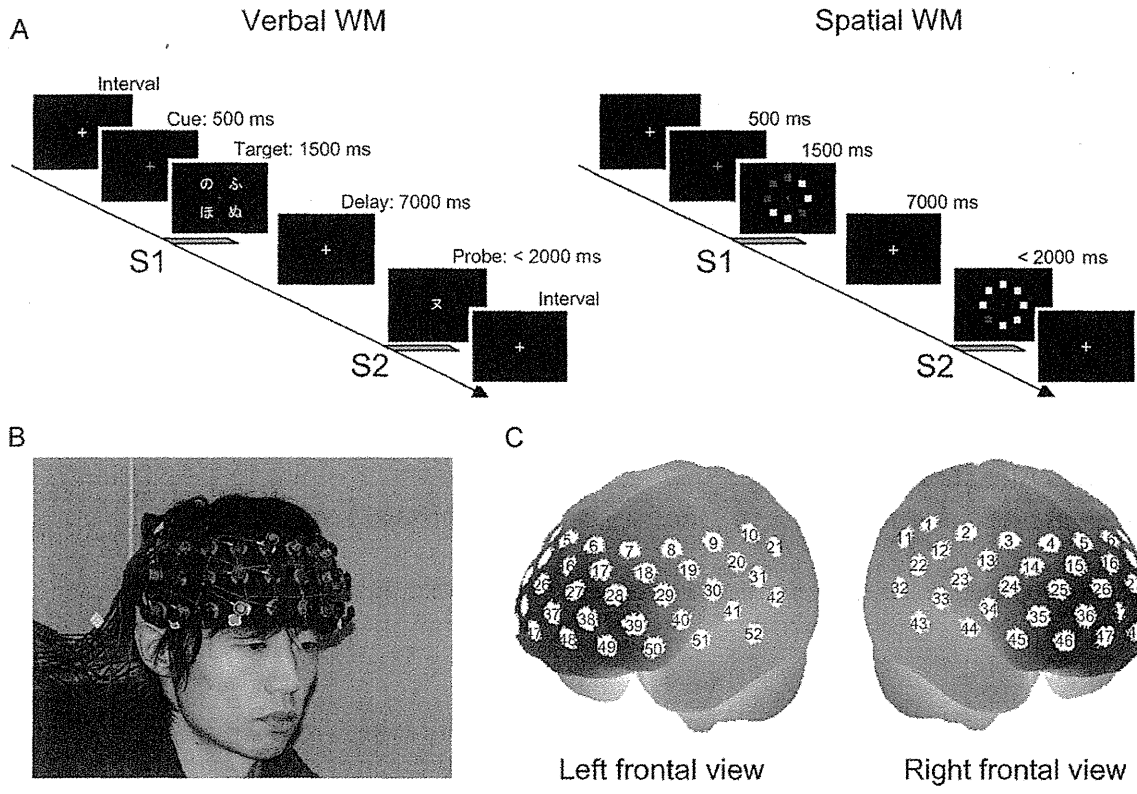

Fig. 1. Task paradigm and experimental setting. (A) Schematic diagrams of verbal and spatial WM tasks. Participants were instructed to remember the target stimuli (S1) and to report whether the character (verbal WM task) or location of a red square (spatial WM task) presented in the probe stimuli (S2) was identical to one of the items in S1. (B) OT probe-holder worn by participant. A 3 × 11 probe array (17 light sources and 16 detectors) was positioned on the forehead. (C) Arrangement of measurement positions (52 channels) in MNI space, which was estimated by means of probabilistic registration method (Singh et al., 2005).

the demand effect exists) depend on various methods of mood induction procedures (Martin, 1990) and may differ qualitatively from those of naturalistic moods. Indeed, a previous study demonstrated that induced moods and naturalistic moods can occasionally exert different, or even opposite, effects on certain aspects of cognitive functions (Parrot and Sabini, 1990). To understand the mood-cognition interaction more thoroughly, evidence from both induced and naturalistic moods should be converged (Mayer et al., 1995). Thus, the relationship between naturalistic mood and WM is worth investigating in neuroimaging studies, in addition to previous research using affective modulation paradigms.

In this study, we investigated whether and how naturalistic moods in healthy adults are associated with PFC activity during WM tasks. We used individual differences (Kosslyn et al., 2002), which enable exploring the relationship between mood and brain activity without any explicit mood induction. Specifically, we tested whether inter-individual variations in the levels of positive or negative moods are correlated with PFC activity in response to the WM tasks. Participants' naturalistic moods in their current life (the last week) were assessed with the Profile of Mood States (McNair et al., 1971; Yokoyama et al., 1990), a self-report questionnaire used in previous studies that examined the PFC role in the mood-cognition interaction (Canli et al., 2004; Harrison et al., 2009). PFC activity during WM tasks was measured with optical topography (OT), a non-invasive, low-constraint neuroimaging technique, to minimize the mood modulation due to the experiment. OT enables measuring hemodynamic responses in the cerebral cortex under near-natural situations (e.g., sitting position) (Maki et al., 1995; Tsujimoto et al., 2004) and can tap into relationships between naturalistic mood and PFC activity (Suda et al., 2009; Suda et al., 2008). We used two types of WM tasks (verbal and spatial) that had an identical delayed-response paradigm, a standard cognitive activation paradigm often used in the human neuroimaging studies of WM (Smith and Jonides, 1999; Smith et al., 1996).

2. Materials and methods

2.1. Participants

Thirty-two healthy adults participated in the experiment after they provided written informed consent. Their handedness was assessed with the Edinburgh Handedness Inventory (Oldfield, 1971), and data from a female who demonstrated left-handedness were excluded from the analysis. Data from two other females were also excluded from the analysis because of their poor behavioral performance (<50% correct responses for the spatial WM tasks). The remaining 29 participants (12 females, 17 males, mean age = 35.9 years, SD = 7.7, and range = 25–58, all right handed) were included in the final analysis. The study was approved by the Ethics Committee of Hitachi, Ltd.

2.2. Mood assessment

The participants' naturalistic moods were assessed by means of a short form of the Profile of Mood States (McNair et al., 1971), which has been translated and validated for the Japanese general population (Yokoyama et al., 1990). McNair et al. (1971) defined moods as mild, pervasive, and generalized affective states that are perceived subjectively by individuals. The participants rated 30 mood-related adjectives on a 5-point scale ranging from 0 ("not at all") to 4 ("extremely") on the basis of how they had been feeling during the past week. While the POMS consists of six identifiable mood factors (tension, depression, anger, vigor, fatigue, and confusion), our study focused on the POMS positive mood score (the score of vigor subscale) and the POMS negative mood score (the sum of the score for the other five subscales), following a previous study (Canli et al., 2004).

2.3. WM tasks

The tasks were presented through software, the Platform of Stimuli and Tasks (developed by Hitachi, ARL). Each participant performed two types of WM tasks (verbal and spatial), which had an identical delayed-response paradigm (Fig. 1A). In both tasks, each trial started with a 1500-ms presentation of the target stimuli (S1), which was followed by a delay of 7000 ms. A probe stimulus (S2) was then presented for 2000 ms or until the participant responded. The intervals between S2 onset and the following S1 onset in the next trial were randomized from 16 to 24 s. Only a

fixation cross was presented during the interval and the delay period. In addition, a visual cue (changing the color of the fixation cross) was presented for 500 ms prior to trial onset. Auditory cues (1000 and 800 Hz pure tones of 100-ms duration) were presented at the onsets of the visual cue and S2, respectively.

In the verbal WM task, four Japanese characters in *Hiragana* were presented as S1, and a Japanese character in *Katakana* was presented as S2. The participants were instructed to judge whether the character presented as S2 corresponded to any of the characters in S1 and then to press the appropriate button. Because the characters in S1 and S2 were presented in different Japanese morphograms (i.e., *Hiragana/Katakana*), participants were prompted to make their judgments based on the phonetic information of the characters, not by their form. In the spatial WM task, S1 was the location of four red squares out of eight locations, and S2 was the location of a red square. The participants' task was to assess if the location of the red square presented as S2 was identical to any of the locations of the four red squares presented in S1.

Each WM task had two additional conditions: Eriksen flanker tasks (Eriksen and Eriksen, 1974) were embedded in the delay period as distracter stimuli. These conditions were irrelevant to the purpose of the present study, so they were not included in the analysis.

2.4. Procedure

Participants were seated in a comfortable chair in a dim, quiet room. Their moods were assessed with a short form of the POMS questionnaire (Japanese version) (Yokoyama et al., 1990) at the beginning of the experiment. Next, they received computer-automated instructions that were followed by a brief practice session to familiarize them with the tasks. Thereafter, OT measurements were conducted while the participants performed the WM tasks. The tasks were organized into two sessions, one for the verbal WM task and the other for the spatial WM task, with a counterbalanced order across participants. Each session included five trials of either one of the tasks, and the sessions were separated by a short break (approximately 1 min). After the measurements, the participants completed a brief questionnaire that assessed their feelings about the experiments, which included subjective ratings of task difficulty on a 5-point scale, ranging from 1 ("not at all") to 5 ("extremely"). The duration of the OT measurements was approximately 15 min, and the whole experiment took about 45 min.

2.5. OT measurement

We used an OT system (ETG-4000, Hitachi Medical Corporation, Japan) equipped with 17 near-infrared light sources and 16 detectors. The light sources consisted of near-infrared continuous laser diodes with two wavelengths of 695 and 830 nm. The transmitted light was detected every 100 ms with avalanche photodiodes located 30 mm from the sources. These optodes (i.e., sources and detectors) were arrayed in a 3×11 lattice pattern and embedded in a soft silicon holder that was placed on the participant's forehead (Fig. 1B). This configuration formed 52 measurement points (defined as channels (Chs)), corresponding to each source-detector pair (Fig. 1C). The average power of each light source was 2 mW (for both wavelengths), and the sources were modulated at different frequencies (1–10 kHz) for wavelengths and sources so that signals from different measurement points could be discriminated.

To estimate the locations of the OT channels in the Montreal Neurological Institute (MNI) space and to generate 3-D topographical maps (Figs. 2 and 3), we used the probabilistic registration method (Okamoto and Dan, 2005; Singh et al., 2005). Prior to the experiment, we corrected the sample data for the three-dimensional coordinates of the 33 optode locations and scalp landmarks (in accordance with the international 10–20 system: Fp1, Fp2, Fz, T3, T4, C3, C4) for eight volunteers. The data were recorded with a 3D-magnetic space digitizer (3D probe positioning unit for OT system, EZT-DM101, Hitachi Medical Corporation, Japan).

2.6. Data analysis

Analyses were performed by means of plug-in-based analysis software, Platform for Optical Topography Analysis Tools (developed by Hitachi, ARL; run on MATLAB, The MathWorks, Inc., U.S.A.). First, we calculated the relative values of hemoglobin concentration changes (Hb-signals for oxy-Hb and deoxy-Hb) for each channel on the basis of the modified Beer-Lambert law, using light signals transmitted at the two wavelengths. The time-continuous data of Hb-signals for each channel were separated into task blocks, which were defined as a 25.5-s period starting from 1.0 s before S1 onset and ending 16.0 s after S2 onset, each containing a WM task trial. Next, blocks contaminated by motion artifacts were discarded. Although previous OT studies have used various methods to detect motion artifacts, no established method has been developed. Some studies used subjective methods based on visual inspection (Minagawa-Kawai et al., 2011), whereas others used objective methods (Orihuela-Espina et al., 2010; Takizawa et al., 2008). In this study, we used a criterion similar to (Pena et al., 2003): an oxy-Hb signal change larger than 0.4 mM mm over two successive samples (during 200 ms) was defined as a motion artifact. We found that this criterion effectively detected sharp noises (putatively unphysiological signal changes) identified by a visual inspection in our data, while maintaining the rejection rate at a low level (4.9%). The remaining data were baseline-corrected by linear regression based on the least squares method by using the data for the first 1.0 s the last 4.0 s of each block.

To evaluate the PFC activity during the tasks, we determined the '*activation period*' as being 3.5 s starting 5.0 s after S1 onset and ending on S2 onset (Fig. 2C). The onset of the activation period (5.0 s after S1 onset) was determined by taking into consideration the delay in hemodynamic changes from the neuronal activity. The offset of the activation period (immediately before S1 onset) was selected to avoid any confounding effects related to S2 presentation and the participant's response to the task. Because the activation period was entirely included in the 7.0-s WM-delay period, we expected that Hb-signals during this period would reflect cortical activity related to WM functions (i.e., encoding and maintenance) without it being affected by activity related to visual stimulation due to S2 or by body movement due to pressing buttons. Note that this time window was determined *a priori* and that the results reported here were not changed when we selected a longer time period (e.g., 5.0-s period starting 5.0 s after S1 onset; See Supplementary Fig. S1). The mean signal changes during the activation period, termed '*activation values*,' were calculated for both oxy-Hb and deoxy-Hb signals for each block. To assess the statistical significance of Hb-signal changes for the tasks, we first averaged the activation values within participants then performed a *t*-test (one sample, one-tailed) of the individual activation values against 0 across participants. For the between-task comparison of the activation values, we used a paired *t*-test (two-tailed) across participants.

To analyze the relationships of mood with task performance and PFC activity, we calculated the correlations between the POMS scores and behavioral measures or oxy-Hb signal changes for both WM tasks. We used Spearman's rank correlation because the relationships of subjective ratings with behavioral and neural measures are not necessarily regarded as linear (Schroeter et al., 2004).

All of these statistical analyses were performed for each channel. Therefore, when creating the statistical parametric map consisting of 52 channels, we used the false discovery rate (FDR) method to correct for multiple comparisons (Singh and Dan, 2006) with a threshold of FDR (q) < 0.05. Because FDR correction set a statistical threshold for each analysis, uncorrected *P*-values at thresholds were different across maps. Thus, the ranges of the statistical values (Student's *t* and Spearman's *r*, together with the thresholds of the uncorrected *P*-values) for the significant channels are presented for each statistical parametric map. Note that *P* denotes the uncorrected *P*-values for each channel and that q denotes the FDR for each map throughout this paper.

3. Results

3.1. POMS scores and subjective ratings

The mean and standard deviation (SD) of the POMS positive mood scores and negative mood scores were 8.76 ± 2.89 (ranging from 5 to 16) and 24.8 ± 14.5 (ranging from 3 to 56), respectively. These results are comparable to those obtained for a large sample of healthy Japanese adults (Yokoyama et al., 1990). The scores for male (9.18 ± 3.38 for positive mood scores, 22.8 ± 15.2 for negative mood scores) and female (8.17 ± 2.00 for positive mood scores, 27.6 ± 13.5 for negative mood scores) participants were not significantly different ($P = 0.556$ for positive mood scores, $P = 0.370$ for negative mood scores; Mann–Whitney *U*-test). The POMS positive mood scores and negative mood scores were not significantly correlated ($r = -0.28$, $P = 0.136$; Spearman's rank correlation).

The subjective ratings of task difficulty were 2.62 ± 0.90 for the verbal WM task and 2.93 ± 1.13 for the spatial WM task. The between-task difference was not significant ($P = 0.079$, Wilcoxon signed-rank test).

3.2. Behavioral performances

The mean reaction time (RT) for correct responses within individual participants was calculated for each WM task. The across-participants' mean and SD for RT were 1380 ± 239 ms for the verbal WM task and 1475 ± 270 ms for the spatial WM task. There were no significant differences between tasks ($t = -1.66$, $P = 0.108$, two-tailed paired *t*-test).

The number of correct responses ranged from three to five for both tasks, and the across-participants' mean and SD were 4.72 ± 0.59 for the verbal WM task and 4.31 ± 0.66 for the spatial WM task. Although this difference was relatively small (0.41), it was statistically significant ($P = 0.018$, Wilcoxon signed-rank test).

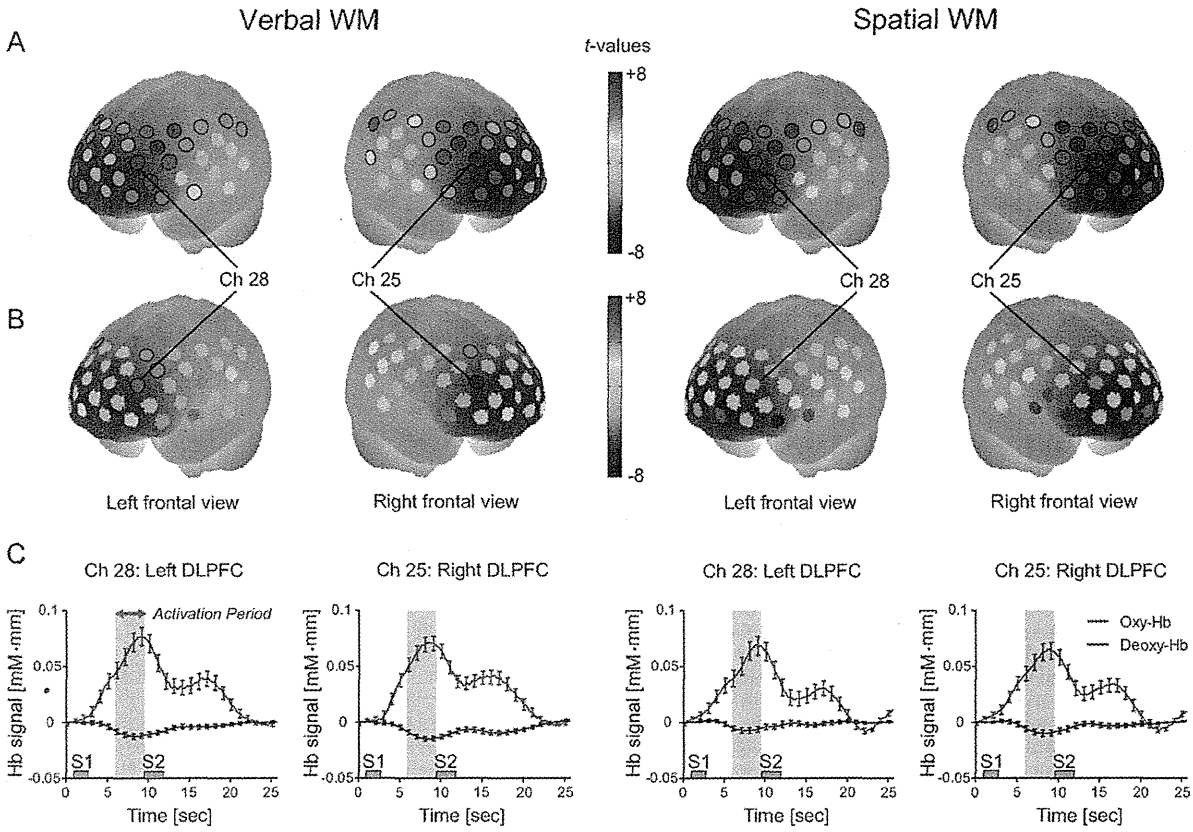

Fig. 2. Hemodynamic changes during verbal and spatial WM tasks. (A) Activation *t*-maps of oxy-Hb signal increase. (B) Activation *t*-maps of deoxy-Hb signal decrease. The Student's *t*-value is indicated by a color scale for each channel. Channels with significant *t*-values are marked with circles (FDR $q < 0.05$). (C) Time courses for Hb-signal changes for representative channels (Chs 25 and 28 for right and left hemispheres, respectively). These time courses represent the grand average (with standard error bars) across all participants. The time spans (green bars perpendicular to *x*-axis) indicate activation period (3.5-s duration). Small rectangles (gray) indicate stimuli presentation time (S1, S2).

To determine whether participants' moods were associated with task performance, we calculated the correlation coefficients (Spearman's *r*) between the POMS scores and behavioral measures (accuracy and RT). A significant correlation was found only in the relationship between the POMS negative mood scores and RT for the verbal WM ($r = -0.37$, $P = 0.046$), although this relationship was no longer significant after controlling for participants' age and gender ($r = -0.29$, $P = 0.141$). No other significant correlation was evident between the POMS scores and behavioral measures ($r = -0.26$ to 0.20, $P > 0.174$; see Supplementary Table).

3.3. PFC activity during WM tasks

First, we examined the across-participants' mean of the activation values for each WM task, without considering individual differences in the mood scores.

For both tasks, significant increases in the oxy-Hb signals (FDR $q < 0.05$) were observed in a broad region of the PFC (Fig. 2A). For the verbal WM task, the oxy-Hb signals increased for 39 channels ($t = 1.97$ to 6.55, $P < 0.030$, $q < 0.05$). Similarly, for the spatial WM task, the oxy-Hb signals increased for 36 channels ($t = 2.10$ to 6.52, $P < 0.024$, $q < 0.05$).

Decreases in the deoxy-Hb signals were observed in a more localized region (Fig. 2B). For the verbal WM task, significant deoxy-Hb signal decreases were observed for five channels (Chs 25, 28, 18, 4, and 7; $t = -5.17$ to -3.03, $P < 0.003$, $q < 0.05$), two for the right hemisphere (Chs 4 and 25), and three for the left hemisphere (Chs 7, 18, and 28). The deoxy-Hb signal decreases for the spatial WM task were not significant at the FDR-corrected threshold. However, for reference, we found considerable decreases in the deoxy-Hb signals for the five channels (Chs 25, 18, 4, 8, and 28; $t = -2.82$ to -1.71, $P < 0.05$ but $q > 0.05$), two for the right hemisphere (Chs 4 and 25), and three for the left hemisphere (Chs 8, 18, and 28).

A comparison of the activation values between the verbal and spatial WM tasks revealed no significant differences in either the oxy-Hb signal increases or the deoxy-Hb signal decreases ($q > 0.05$).

3.4. Temporal characteristics of oxy-Hb signal change

We analyzed the temporal characteristics of the oxy-Hb signal change based on the grand-averaged time course (Fig. 2C). For the channels where the oxy-Hb signal increases were significant during the activation period, the time courses for the oxy-Hb signal change had two peaks. The first (and the maximum) peak was observed during the delay period, and the second, more modest peak was observed after S2 was presented. We calculated the peak latency for the first peak, which was defined as the duration from S1 onset to the time the oxy-Hb signal reached a maximal value, and averaged this across channels with a significant oxy-Hb signal increase for both WM tasks. The mean of the peak latency was 7.81 ± 0.90 s for the verbal WM task and 7.61 ± 1.08 s for the spatial WM task. The difference between tasks was not significant ($t = 1.82$, $df = 35$, $P = 0.077$, two-tailed paired *t*-test).

3.5. Correlation of POMS score with PFC activity

Next, to examine how the participants' moods were associated with the PFC activity during each WM task, we analyzed the correlation (Spearman's rank correlation) between the POMS scores

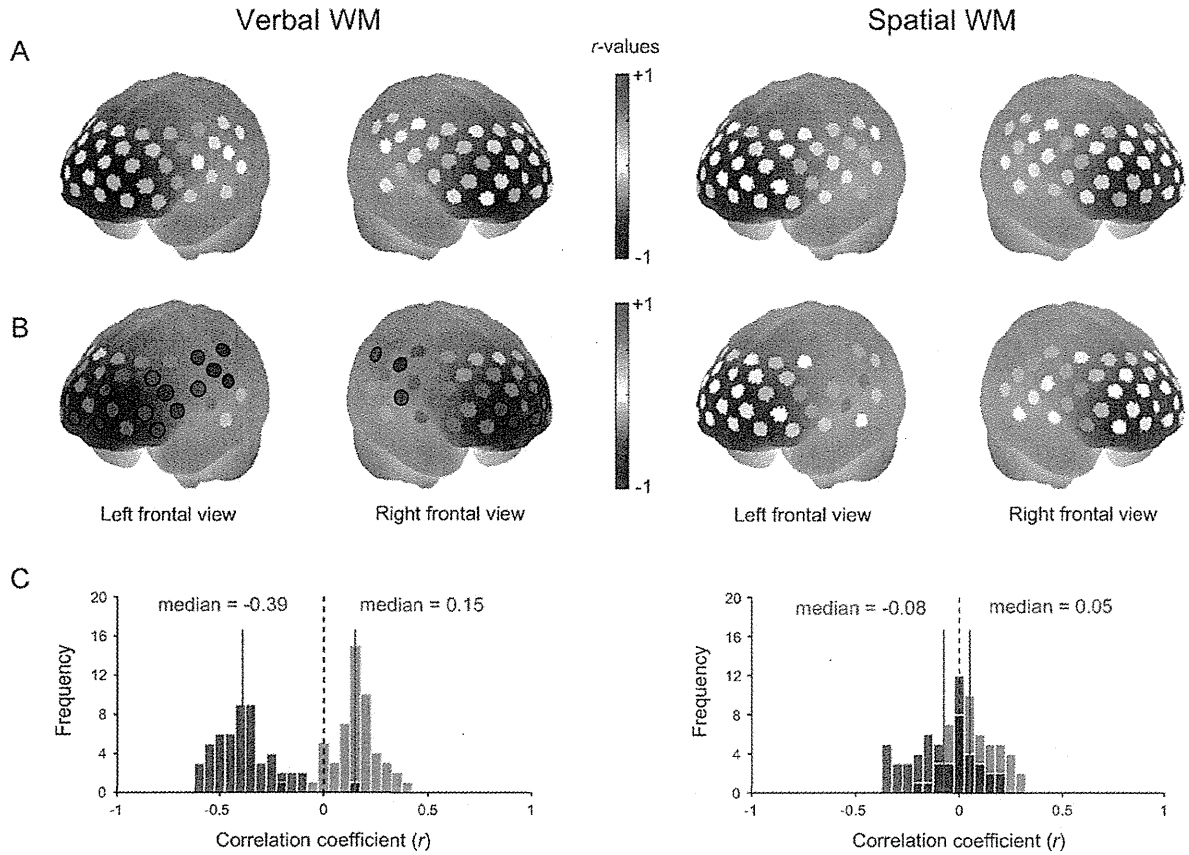

Fig. 3. Correlation between POMS scores and oxy-Hb signals. (A) Correlation *r*-maps showing relationship between POMS positive mood scores and oxy-Hb signal increase. (B) Correlation *r*-maps showing relationship between POMS negative mood scores and oxy-Hb signal increase. Left pairs: verbal WM task, right pairs: spatial WM task. The correlation coefficient (Spearman's *r*) is indicated by a color scale for each channel. Channels with statistical significance are marked with circles (FDR $q < 0.05$). (C) Histograms illustrate distributions of *r*-values for each *r*-map (Left: verbal WM, right: spatial WM). The vertical line indicates the median *r*-value among 52 channels consisting of a map. Red: correlation with POMS positive mood score, blue: correlation with POMS negative mood score.

and the activation values. We used only the oxy-Hb signal change because the deoxy-Hb signals did not show clear changes compared to the oxy-Hb signals (as described before).

For the verbal WM task, the oxy-Hb signal changes during the task tended to be positively correlated with the POMS positive mood scores (median *r*-value = 0.15, ranging from −0.21 to 0.40), whereas negatively correlated with the POMS negative mood scores (median *r*-value = −0.39, ranging from −0.62 to 0.16) (Fig. 3). We found statistically significant negative correlations between the POMS negative mood scores and the oxy-Hb signal changes for 19 channels ($r = -0.62$ to -0.44, $P = 0.0006$ to 0.017, $q < 0.05$) (Fig. 3B). Notably, the partial correlation analysis showed that a significant correlation remained in a specific channel (Ch 28; $r = -0.62$, $P = 0.0009$, $q < 0.05$) even when the participants' age, gender, and task performance (accuracy and RT) were controlled for. In addition, the correlation coefficients for the male ($n = 17$) and female ($n = 12$) participants were not significantly different in this channel ($r = -0.49$ for males, $r = -0.53$ for females; $P = 0.913$, Fisher's *Z*-test). The correlation plot for Ch 28 is shown in Fig. 4.

For the spatial WM task, the oxy-Hb signal changes during the task did not significantly correlate with either the POMS positive mood scores ($r = -0.20$ to 0.30, $P > 0.116$, $q > 0.05$) or negative mood scores ($r = -0.37$ to 0.21, $P > 0.056$, $q > 0.05$).

We also examined the correlations between task performance (accuracy and RT) and the oxy-Hb signal changes. Although there was a weak trend that higher accuracy was associated with a larger oxy-Hb increase in the frontopolar region for both verbal and spatial WM tasks ($r < 0.35$), no significant relationship was found (Supplementary Fig. S2).

4. Discussion

We measured the PFC activity during verbal and spatial WM tasks under low-constraint, near-natural conditions by using OT,

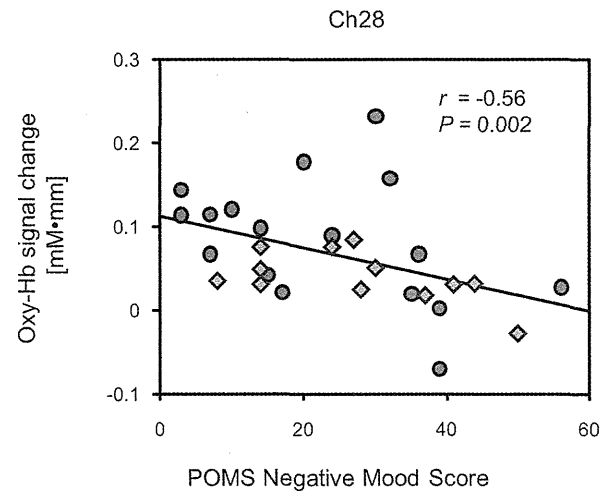

Fig. 4. Scatter plot showing relationship between POMS negative mood scores and PFC activity during verbal WM task in Ch 28. The negative correlation between the POMS scores and PFC activity was significant (FDR $q < 0.05$) in this channel, even after controlling for age, gender, and task performance. The blue circles indicate male participants, and the red diamonds indicate female participants. *r*: Spearman's rank correlation coefficient, *P*: uncorrected value. (For interpretation of the color information in this figure legend, the reader is referred to the web version of the article.)

to investigate the relationships between naturalistic mood and PFC activity. The results revealed statistically significant negative correlations between the POMS negative mood scores and PFC activity during the verbal WM task, whereas the opposite tendency was found for the POMS positive mood scores. However, the PFC activity during the task was not significantly correlated with either the POMS positive or negative mood scores for the spatial WM task. Our results indicate that even a normal range of mood variation in healthy individuals is associated with PFC activity during a WM task, suggesting a mood-cognition interaction under everyday circumstances manifested in PFC activity.

4.1. PFC activity induced by WM tasks

We observed a significant oxy-Hb signal increase in the PFC region in response to both verbal and spatial WM tasks. We did not observe a clear deoxy-Hb signal decrease comparable to the oxy-Hb signal increase, probably due to the lower signal to noise ratio. The decrease in the deoxy-Hb signal was significant only for the verbal WM task, but a similar spatial pattern was observed for the spatial WM task (Fig. 2B). An oxy-Hb signal increase accompanied by a deoxy-Hb signal decrease is considered to be a typical pattern of a hemodynamic response elicited by neuronal activity often observed in OT measurements (Herrmann et al., 2007; Sato et al., 2005, 1999). This pattern was found in the bilateral dorsolateral PFC, as identified by the probabilistic registration method (Okamoto and Dan, 2005; Singh et al., 2005). Therefore, we regarded these areas as activation foci responsible for WM functions. These results are consistent with those from previous research with other modalities (such as fMRI and PET), which have demonstrated DLPFC activation in response to performance of WM tasks (Gray et al., 2002; Smith and Jonides, 1999). Previous OT studies have also reported DLPFC activation during WM tasks (Hoshi et al., 2003; Tsujimoto et al., 2004). In particular, Tsujimoto et al. (2004), using the same delayed-response paradigm for the spatial WM task in our study, found that the oxy-Hb signal increase during the delay period was indeed WM-load dependent (two items vs. four items). This finding also supports that the PFC activity observed in our study can be regarded as WM related.

The PFC activity in response to the WM tasks was similar across the tasks not only in the spatial activation pattern (Fig. 2A and B) but also in the temporal characteristics (Fig. 2C), as shown by the analysis on peak latency. Although some previous studies found laterality in the PFC activity between verbal and spatial WM (Smith and Jonides, 1999; Smith et al., 1996) (i.e., relatively right dominant activation in spatial WM and left dominant activation in verbal WM), we did not observe significant differences in PFC activity between the tasks. One reason for this might be that we used a small number of trials for each condition, resulting in less sensitivity to differences in cortical responses between tasks. Whether OT can detect the lateralized PFC activity related to WM functions is a future issue to be investigated.

4.2. Relationship between negative mood and PFC activity associated with WM

We found a significant negative correlation between the POMS negative mood scores and the oxy-Hb signal increases—participants with higher levels of negative moods showed lower levels of PFC activity specifically during the verbal WM task. Of importance, this relationship was not explained by potential confounding factors such as age, gender, or task performance (i.e., accuracy and RT), as determined by partial correlation analysis. Particularly, the significant result in the partial correlation analysis was obtained in a channel located in the left DLPFC (Ch 28), where the WM-related activity (characterized by both the significant increase in the oxy-Hb signal and the significant decrease in the deoxy-Hb signal) was observed in the group-average analysis. Our results are consistent with the previous fMRI study by Qin et al. (2009), who reported that an induced negative mood attenuated DLPFC activity during a verbal WM task (numerical N-back task). The present study suggests that not only an induced negative mood but also a naturalistic negative mood is associated with PFC activity related to verbal WM function. Our results extend previous neuroimaging findings regarding the mood-cognition interaction to broader context under everyday circumstances: subjective moods during recent life situations are reflected in PFC activity responsive to cognitive tasks. The use of a low-constraint, less-stressful neuroimaging tool as well as a relatively short measurement time might have enabled us to probe the relationship between naturalistic mood and PFC activity sensitively.

We did not observe a significant association between performance (accuracy or RT) and mood scores or OT signals. Thus, it is unclear whether lower levels of PFC activity in participants reporting higher levels of negative moods indicate impoverished PFC reactivity to verbal WM or greater processing efficiency for verbal WM. However, we emphasize that our results are in line with previous OT studies showing that PFC activity during verbal fluency tasks is decreased in people who have higher levels of fatigue and sleepiness, apart from task performance (i.e., the effect of task performance on PFC activity was adjusted by multiple regression) (Suda et al., 2009, 2008). Collectively, these results including ours suggest that decreased PFC activity is a neural marker of higher negative mood (or lower motivation to engage in cognitive tasks), which could be more sensitive than behavioral measures. A more reliable relationship between behavioral measures and mood scores or PFC activity might be obtained if we increase the number of trials or use more difficult cognitive tasks.

One of the advantages of our study compared to the previous OT studies showing negative associations between PFC activity and levels of fatigue and sleepiness (Suda et al., 2009; Suda et al., 2008) is the use of a simple cognitive task, well described in the previous neuroimaging studies and requiring minimum motor responses. While verbal fluency tasks are useful tools for clinical research (Kameyama et al., 2006; Suto et al., 2004; Takizawa et al., 2008), these tasks involve many cognitive processes (e.g., word generation, verbal WM, and cognitive flexibility), making it difficult to characterize what aspects of cognitive processes are indeed relevant to decreased PFC activity associated with negative moods. Our study provides clearer evidence that the PFC is involved in the interaction between naturalistic mood and verbal WM.

We found a significant correlation between mood and PFC activity only for the verbal WM task but not for the spatial WM task. This result could imply that the relationship between mood and PFC activity differs across cognitive functions. Interestingly, some studies have reported that positive and negative moods are differently linked with verbal and spatial cognitive functions (Bartolic et al., 1999; Papousek et al., 2009). In these studies, performances on verbal fluency tasks were relatively worse than those on non-verbal (figural) fluency tasks in negative (dysphoric or withdrawal-related) moods, but opposite in positive (euphoric or approach-related) moods. These results are consistent with our results that showed the negative correlation between negative mood and PFC activity (as well as the trend of positive correlation between positive mood and PFC activity) if we interpret that higher PFC activity corresponds to better cognitive function (see Supplementary Fig. S2). Other studies using WM tasks also showed that verbal and spatial WM functions are selectively associated with experimentally induced positive or negative moods (Gray, 2001; Gray et al., 2002; Shackman et al., 2006). Considering these studies, our results suggest a specific interaction between negative mood and verbal WM under everyday circumstances.

Although the previous studies reported the selective association of mood with spatial WM in an opposite manner to that with verbal WM (Bartolic et al., 1999; Gray, 2001), we did not observed a significant relationship between mood and PFC activity for the spatial WM task. One possibility causing this result is the individual variations in strategy use during the spatial WM task. In the verbal WM task, we used different Japanese morphograms (i.e., Hiragana/Katakana) for target (S1) and probe (S2) stimuli to prompt participants to use a verbal-phonological strategy rather than a visuospatial strategy (Smith et al., 1996). However, the spatial WM task used in our study allowed participants to use either a verbal or spatial strategy because the location of the target stimuli can be remembered by verbal labels (e.g., a number corresponding to each location), as discussed in previous studies (Nystrom et al., 2000). Cortical recruitment during WM tasks is known to depend on strategy use (Glabus et al., 2003). Thus, the homogeneity of strategy use (verbal or spatial) across participants conceivably made the relationship between mood and PFC activity unclear for the spatial WM task. One potential solution is to control the strategy use across participants in future research by using different task paradigms or by providing explicit instructions for memory strategy.

The underlying neural mechanisms of the selective interaction between mood and cognition are still unclear. Some researchers have proposed a "prefrontal asymmetry" hypothesis (Gray, 2001; Gray et al., 2002; Shackman et al., 2006). This hypothesis argues that positive (approach-related) and negative (withdrawal-related) affects are predominantly associated with the left and right hemispheres, respectively, whereby different affects are selectively related to cognitive functions linked with each hemisphere (e.g., verbal-left and spatial-right). However, incorporating our results with this hypothesis is difficult because we did not find clear evidence suggesting hemispheric asymmetry. Another account of the selective interaction between mood and cognition is based on pharmacological evidence. Animal studies have shown that certain cognitive functions involving the PFC (e.g., attentional set-shifting and reversal learning) are distinctly controlled by different neurotransmitters such as dopamine and serotonin (Robbins and Roberts, 2007). Because dopamine and serotonin have been suggested to be associated with positive and negative moods (Mitchell and Phillips, 2007), these transmitters could intermediate the selective interaction between moods and cognitive functions.

It should be noted that previous findings concerning the difference in mood-cognition interaction across cognitive functions remain inconsistent, possibly resulting from the variances in the task paradigms and the mood induction procedures (Shackman et al., 2006). In addition, we found a small but significant difference in accuracy between the tasks, suggesting slightly higher difficulty in the spatial WM tasks than the verbal WM task. This makes it difficult to interpret why we observed the between-task difference in the relationship between mood and PFC activity. Further investigation is needed to illuminate the possible difference between verbal and spatial WM in relation to mood under natural circumstances.

4.3. Limitations

Although we showed that the correlation between negative mood and the PFC activity during the verbal WM task was significant after controlling for age, gender, and task performance, several other factors could still mediate the relationship between mood and PFC activity. For example, this study did not assess or control participants' intelligence. Measures such as intelligence quotient (IQ) or fluid intelligence (gF) are known to be associated with both mood states and PFC activity during WM tasks (Gray et al., 2003; Samuel, 1980). These studies have shown that higher IQ is associated with lower negative moods and that greater gF is associated with more PFC activation during WM tasks. Thus, our results could imply that higher intelligence mediates an inverse relationship between negative moods and PFC activation during the verbal WM task. Another concern is the relationship between naturalistic moods and personality traits. The experimental framework of the present study (i.e., individual-differences approach) precludes us from determining whether the observed relationship between mood and PFC activity derived from state-dependent factors (day-to-day fluctuations in mood states within an individual) or trait-like factors ('*dispositional moods*' persistent across time). Although the POMS questionnaire we used to evaluate the participants' naturalistic moods is considered to evaluate the responders' typical mood states rather than their personality traits (McNair and Heuchert, 2003), the participants' naturalistic moods under their current life situations may depend on their personality traits (Davidson, 2004; Kosslyn et al., 2002). This does not contradict previous fMRI studies suggesting the link between personality traits and PFC activity in response to WM tasks (DeYoung et al., 2009; Kumari et al., 2004). Meanwhile, several experiments have indicated that mood changes within individuals are indeed associated with PFC activity during cognitive tasks (Harrison et al., 2009; Liston et al., 2009). Thus, state-dependent mood factors apart from individual trait factors might at least in part have contributed to our results. To dissociate the contributions of state and trait factors to PFC activity, we need to administer multiple questionnaires for both state and trait measurement (Canli et al., 2004) or to use a within-subject design in which the PFC activity of individual participants is measured over multiple occasions.

5. Conclusion

Our study demonstrated that naturalistic moods in healthy people are related to PFC activity during a verbal WM task. We showed that this relationship remained significant even after controlling for potential confounding factors such as age, gender, and task performance. One thing of note is that a mild variation of naturalistic negative moods among healthy people can be associated with PFC activity even absent experimental affective modulation. The relationship between negative mood and verbal WM in the PFC is particularly of interest, considering clinical findings showing PFC impairment during verbal WM tasks in mood disorders such as major depression (Harvey et al., 2005; Matsuo et al., 2007; Siegle et al., 2007). Further research will lead to more comprehensive understanding of the mood-cognition interaction under broader contexts, bridging the gap across induced moods and naturalistic moods among healthy people, as well as pathological moods in patients with mood disorders.

Acknowledgments

We thank Dr. Akiko Obata and Dr. Hiroaki Kawamichi for their helpful assistance. We also thank Dr. Kisou Kubota for the meaningful discussions we had with him.

Appendix A. Supplementary data

Supplementary data associated with this article can be found, in the online version, at doi:10.1016/j.neures.2011.02.011.

References

Anticevic, A., Repovs, G., Barch, D.M., 2010. Resisting emotional interference: brain regions facilitating working memory performance during negative distraction. Cogn. Affect. Behav. Neurosci. 10, 159–173.

Ashby, F.G., Isen, A.M., Turken, A.U., 1999. A neuropsychological theory of positive affect and its influence on cognition. Psychol. Rev. 106, 529–550.

Baddeley, A., 2003. Working memory: looking back and looking forward. Nat. Rev. Neurosci. 4, 829–839.

Bartolic, E.I., Basso, M.R., Schefft, B.K., Glauser, T., Titanic-Schefft, M., 1999. Effects of experimentally-induced emotional states on frontal lobe cognitive task performance. Neuropsychologia 37, 677–683.
Canli, T., Amin, Z., Haas, B., Omura, K., Constable, R.T., 2004. A double dissociation between mood states and personality traits in the anterior cingulate. Behav. Neurosci. 118, 897–904.
Davidson, R.J., 2004. Well-being and affective style: neural substrates and biobehavioural correlates. Philos. Trans. R. Soc. Lond. B Biol. Sci. 359, 1395–1411.
DeYoung, C.G., Shamosh, N.A., Green, A.E., Braver, T.S., Gray, J.R., 2009. Intellect as distinct from Openness: differences revealed by fMRI of working memory. J. Pers. Soc. Psychol. 97, 883–892.
Eriksen, B.A., Eriksen, C.W., 1974. Effects of noise letters upon the identification of a target letter in a nonsearch task. Percept. Psychophys. 16, 143–149.
Glabus, M.F., Horwitz, B., Holt, J.L., Kohn, P.D., Gerton, B.K., Callicott, J.H., Meyer-Lindenberg, A., Berman, K.F., 2003. Interindividual differences in functional interactions among prefrontal, parietal and parahippocampal regions during working memory. Cereb. Cortex 13, 1352–1361.
Gray, J.R., 2001. Emotional modulation of cognitive control: approach-withdrawal states double-dissociate spatial from verbal two-back task performance. J. Exp. Psychol. Gen. 130, 436–452.
Gray, J.R., Braver, T.S., Raichle, M.E., 2002. Integration of emotion and cognition in the lateral prefrontal cortex. Proc. Natl. Acad. Sci. U.S.A. 99, 4115–4120.
Gray, J.R., Chabris, C.F., Braver, T.S., 2003. Neural mechanisms of general fluid intelligence. Nat. Neurosci. 6, 316–322.
Harrison, N.A., Brydon, L., Walker, C., Gray, M.A., Steptoe, A., Dolan, R.J., Critchley, H.D., 2009. Neural origins of human sickness in interoceptive responses to inflammation. Biol. Psychiatry 66, 415–422.
Harvey, P.O., Fossati, P., Pochon, J.B., Levy, R., Lebastard, G., Lehericy, S., Allilaire, J.F., Dubois, B., 2005. Cognitive control and brain resources in major depression: an fMRI study using the n-back task. NeuroImage 26, 860–869.
Herrmann, M.J., Walter, A., Schreppel, T., Ehlis, A.C., Pauli, P., Lesch, K.P., Fallgatter, A.J., 2007. D4 receptor gene variation modulates activation of prefrontal cortex during working memory. Eur. J. Neurosci. 26, 2713–2718.
Hoshi, Y., Tsou, B.H., Billock, V.A., Tanosaki, M., Iguchi, Y., Shimada, M., Shinba, T., Yamada, Y., Oda, I., 2003. Spatiotemporal characteristics of hemodynamic changes in the human lateral prefrontal cortex during working memory tasks. NeuroImage 20, 1493–1504.
Kameyama, M., Fukuda, M., Yamagishi, Y., Sato, T., Uehara, T., Ito, M., Suto, T., Mikuni, M., 2006. Frontal lobe function in bipolar disorder: a multichannel near-infrared spectroscopy study. NeuroImage 29, 172–184.
Kosslyn, S.M., Cacioppo, J.T., Davidson, R.J., Hugdahl, K., Lovallo, W.R., Spiegel, D., Rose, R., 2002. Bridging psychology and biology. The analysis of individuals in groups. Am. Psychol. 57, 341–351.
Kumari, V., ffytche, D.H., Williams, S.C., Gray, J.A., 2004. Personality predicts brain responses to cognitive demands. J. Neurosci. 24, 10636–10641.
Liston, C., McEwen, B.S., Casey, B.J., 2009. Psychosocial stress reversibly disrupts prefrontal processing and attentional control. Proc. Natl. Acad. Sci. U.S.A. 106, 912–917.
Luciana, M., Collins, P.F., Depue, R.A., 1998. Opposing roles for dopamine and serotonin in the modulation of human spatial working memory functions. Cereb. Cortex 8, 218–226.
Maki, A., Yamashita, Y., Ito, Y., Watanabe, E., Mayanagi, Y., Koizumi, H., 1995. Spatial and temporal analysis of human motor activity using noninvasive NIR topography. Med. Phys. 22, 1997–2005.
Martin, M., 1990. On the induction of mood. Clin. Psychol. Rev. 10, 669–697.
Matsuo, K., Glahn, D.C., Peluso, M.A., Hatch, J.P., Monkul, E.S., Najt, P., Sanches, M., Zamarripa, F., Li, J., Lancaster, J.L., Fox, P.T., Gao, J.H., Soares, J.C., 2007. Prefrontal hyperactivation during working memory task in untreated individuals with major depressive disorder. Mol. Psychiatry 12, 158–166.
Mayer, J.D., McCormick, L.J., Strong, S.E., 1995. Mood-congruent memory and natural mood: new evidence. Pers. Soc. Psychol. Bull. 21, 736–746.
McNair, D.M., Heuchert, J.P., 2003. Profile of Mood States Technical Update. Multi-Health Systems, New York.
McNair, P.M., Lorr, M., Droppleman, L.F., 1971. Profile of Mood States Manual. Educational and Industrial Testing Service, San Diego.
Minagawa-Kawai, Y., van der Lely, H., Ramus, F., Sato, Y., Mazuka, R., Dupoux, E., 2011. Optical brain imaging reveals general auditory and language-specific processing in early infant development. Cereb. Cortex 21, 254–261.
Mitchell, R.L., Phillips, L.H., 2007. The psychological, neurochemical and functional neuroanatomical mediators of the effects of positive and negative mood on executive functions. Neuropsychologia 45, 617–629.
Nystrom, L.E., Braver, T.S., Sabb, F.W., Delgado, M.R., Noll, D.C., Cohen, J.D., 2000. Working memory for letters, shapes, and locations: fMRI evidence against stimulus-based regional organization in human prefrontal cortex. NeuroImage 11, 424–446.
Okamoto, M., Dan, I., 2005. Automated cortical projection of head-surface locations for transcranial functional brain mapping. NeuroImage 26, 18–28.
Oldfield, R.C., 1971. The assessment and analysis of handedness: the Edinburgh inventory. Neuropsychologia 9, 97–113.
Orihuela-Espina, F., Leff, D.R., James, D.R., Darzi, A.W., Yang, G.Z., 2010. Quality control and assurance in functional near infrared spectroscopy (fNIRS) experimentation. Phys. Med. Biol. 55, 3701–3724.
Papousek, I., Schulter, G., Lang, B., 2009. Effects of emotionally contagious films on changes in hemisphere-specific cognitive performance. Emotion 9, 510–519.
Parrot, W.G., Sabini, J., 1990. Mood and memory under natural conditions: evidence for mood incongruent recall. J. Pers. Soc. Psychol. 59, 321–336.
Pena, M., Maki, A., Kovacic, D., Dehaene-Lambertz, G., Koizumi, H., Bouquet, F., Mehler, J., 2003. Sounds and silence: an optical topography study of language recognition at birth. Proc. Natl. Acad. Sci. U.S.A. 100, 11702–11705.
Perlstein, W.M., Elbert, T., Stenger, V.A., 2002. Dissociation in human prefrontal cortex of affective influences on working memory-related activity. Proc. Natl. Acad. Sci. U.S.A. 99, 1736–1741.
Qin, S., Hermans, E.J., van Marle, H.J., Luo, J., Fernandez, G., 2009. Acute psychological stress reduces working memory-related activity in the dorsolateral prefrontal cortex. Biol. Psychiatry 66, 25–32.
Robbins, T.W., Roberts, A.C., 2007. Differential regulation of fronto-executive function by the monoamines and acetylcholine. Cereb. Cortex 17, i151–i160.
Robinson, O.J., Sahakian, B.J., 2009. A double dissociation in the roles of serotonin and mood in healthy subjects. Biol. Psychiatry 65, 89–92.
Samuel, W., 1980. Mood and personality correlates of IQ by race and sex of subject. J. Pers. Soc. Psychol. 38, 993–1004.
Sato, H., Fuchino, Y., Kiguchi, M., Katura, T., Maki, A., Yoro, T., Koizumi, H., 2005. Inter-subject variability of near-infrared spectroscopy signals during sensorimotor cortex activation. J. Biomed. Opt. 10, 44001.
Sato, H., Takeuchi, T., Sakai, K.L., 1999. Temporal cortex activation during speech recognition: an optical topography study. Cognition 73, B55–B66.
Schroeter, M.L., Zysset, S., Wahl, M., von Cramon, D.Y., 2004. Prefrontal activation due to Stroop interference increases during development–an event-related fNIRS study. NeuroImage 23, 1317–1325.
Shackman, A.J., Sarinopoulos, I., Maxwell, J.S., Pizzagalli, D.A., Lavric, A., Davidson, R.J., 2006. Anxiety selectively disrupts visuospatial working memory. Emotion 6, 40–61.
Siegle, G.J., Thompson, W., Carter, C.S., Steinhauer, S.R., Thase, M.E., 2007. Increased amygdala and decreased dorsolateral prefrontal BOLD responses in unipolar depression: related and independent features. Biol. Psychiatry 61, 198–209.
Singh, A.K., Dan, I., 2006. Exploring the false discovery rate in multichannel NIRS. NeuroImage 33, 542–549.
Singh, A.K., Okamoto, M., Dan, H., Jurcak, V., Dan, I., 2005. Spatial registration of multichannel multi-subject fNIRS data to MNI space without MRI. NeuroImage 27, 842–851.
Smith, E.E., Jonides, J., 1999. Storage and executive processes in the frontal lobes. Science 283, 1657–1661.
Smith, E.E., Jonides, J., Koeppe, R.A., 1996. Dissociating verbal and spatial working memory using PET. Cereb. Cortex 6, 11–20.
Suda, M., Fukuda, M., Sato, T., Iwata, S., Song, M., Kameyama, M., Mikuni, M., 2009. Subjective feeling of psychological fatigue is related to decreased reactivity in ventrolateral prefrontal cortex. Brain Res. 1252, 152–160.
Suda, M., Sato, T., Kameyama, M., Ito, M., Suto, T., Yamagishi, Y., Uehara, T., Fukuda, M., Mikuni, M., 2008. Decreased cortical reactivity underlies subjective daytime light sleepiness in healthy subjects: a multichannel near-infrared spectroscopy study. Neurosci. Res. 60, 319–326.
Suto, T., Fukuda, M., Ito, M., Uehara, T., Mikuni, M., 2004. Multichannel near-infrared spectroscopy in depression and schizophrenia: cognitive brain activation study. Biol. Psychiatry 55, 501–511.
Takizawa, R., Kasai, K., Kawakubo, Y., Marumo, K., Kawasaki, S., Yamasue, H., Fukuda, M., 2008. Reduced frontopolar activation during verbal fluency task in schizophrenia: a multi-channel near-infrared spectroscopy study. Schizophr. Res. 99, 250–262.
Tsujimoto, S., Yamamoto, T., Kawaguchi, H., Koizumi, H., Sawaguchi, T., 2004. Prefrontal cortical activation associated with working memory in adults and preschool children: an event-related optical topography study. Cereb. Cortex 14, 703–712.
Yokoyama, K., Araki, S., Kawakami, N., Takeshita, T., 1990. Production of the Japanese edition of profile of mood states (POMS): assessment of reliability and validity. Nippon Koshu Eisei Zasshi 37, 913–918.

Journal of Biomedical Optics 16(12), 126007 (December 2011)

Correlation of within-individual fluctuation of depressed mood with prefrontal cortex activity during verbal working memory task: optical topography study

Hiroki Sato,[a,*] Ryuta Aoki,[b,c,*] Takusige Katura,[a] Ryoichi Matsuda,[b] and Hideaki Koizumi[a]
[a]Hitachi, Ltd., Central Research Laboratory, 2520 Akanuma, Hatoyama, Saitama 350-0395, Japan
[b]The University of Tokyo, Graduate School of Arts and Sciences, 3-8-1 Komaba, Meguro-ku, Tokyo 153-8902, Japan
[c]Japan Society for the Promotion of Science, 8 Ichibancho, Chiyoda-ku, Tokyo 102-8472, Japan

Abstract. Previous studies showed that interindividual variations in mood state are associated with prefrontal cortex (PFC) activity. In this study, we focused on the depressed-mood state under natural circumstances and examined the relationship between within-individual changes over time in this mood state and PFC activity. We used optical topography (OT), a functional imaging technique based on near-infrared spectroscopy, to measure PFC activity for each participant in three experimental sessions repeated at 2-week intervals. In each session, the participants completed a self-report questionnaire of mood state and underwent OT measurement while performing verbal and spatial working memory (WM) tasks. The results showed that changes in the depressed-mood score between successive sessions were negatively correlated with those in the left PFC activation for the verbal WM task ($\rho = -0.56$, $p < 0.05$). In contrast, the PFC activation for the spatial WM task did not co-vary with participants' mood changes. We thus demonstrated that PFC activity during a verbal WM task varies depending on the participant's depressed mood state, independent of trait factors. This suggests that using optical topography to measure PFC activity during a verbal WM task can be used as a potential state marker for an individual's depressed mood state. [DOI: 10.1117/1.3662448]

Keywords: depressed mood; working memory; prefrontal cortex; near-infrared spectroscopy; optical topography; profile of mood states.

Paper 11243R received May 17, 2011; revised manuscript received Oct. 20, 2011; accepted for publication Oct. 25, 2011; published online Nov. 28, 2011.

1 Introduction

The relationship between mood and cognition, as well as the neural mechanisms supporting it, has long attracted researchers in psychology and neuroscience.[1,2] Behavioral experiments have shown that even mild variations in mood state influence various cognitive functions such as working memory (WM) and cognitive fluency.[1,3,4] Recent neuroimaging studies have implicated the prefrontal cortex (PFC) as one of the key regions that converges mood and cognition in the brain.[1,2] For instance, functional magnetic resonance imaging (fMRI) studies have reported that experimentally induced negative moods affect PFC activity during cognitive tasks such as WM and Stroop tasks.[5,6] In addition, near-infrared spectroscopy (NIRS) studies focusing on moods under natural circumstances indicate that people having a high level of fatigue or sleepiness showed decreased PFC activity in response to verbal fluency tasks.[7,8] However, little is known about how PFC activity during cognitive tasks and natural moods, which can vary across days or weeks, are coupled within individuals. Thus, tracking within-individual fluctuations in natural mood and PFC activity during cognitive tasks is necessary to deepen our knowledge about their relationship.

In our previous study, we used optical topography (OT), which is a noninvasive functional imaging-technique based on NIRS,[9–11] to show that a variation in the negative mood state across participants is correlated with their PFC activity for a verbal WM task.[12] OT measures hemodynamic responses in the cerebral cortex under near-natural situations (e.g., sitting position) and allows us to minimize mood modulation due to the experiment itself. In the previous study, the participants' natural moods were assessed by using the Profile of Mood States (POMS), a self-reporting questionnaire.[13,14] As the POMS is used to evaluate a responder's typical mood states rather than personality traits,[15] one can assume that the observed correlation would reflect a state-dependent effect. However, because of the experimental design used in the previous study, i.e., across-subject design, we could not deny the possibility of the contribution of individual trait factors (e.g., personality traits or dispositional moods) in the results.

One solution to dissociate the state-dependent effect found in the previous study[12] from certain trait factors is examining whether PFC activity changes in correlation with his/her mood state using a within-individual design. In this study, we repeated three experiment sessions for each participant at 2-week intervals to trace the time-to-time mood fluctuations within individuals, which enabled us to identify the contribution of each participant's depressed mood state to the variations in their PFC activity independent of trait factors.

*These authors contributed equally to this work.

Address all correspondence to: Hiroki Sato, Hitachi, Ltd., Central Reseach Laboratory, 2520 Akanuma, Hatoyama, Saitama 350-0395 Japan; Tel: +81-492-96-6111; Fax: +81-492-96-5999; E-mail: hiroki.sato.ry@hitachi.com.

1083-3668/2011/16(12)/126007/7/$25.00 © 2011 SPIE

2 Materials and Methods

2.1 *Participants*

Seventeen healthy adults (12 males and 5 females; 25 to 48 years old) participated in the three experimental sessions at 2-week intervals. None of the participants had participated in our previous study.[12] This study was approved by the Ethics Committee of Hitachi, Ltd., and all participants provided written informed consent before the experiments.

2.2 *Mood Assessment*

At the beginning of each session, the participants' natural moods were assessed with a short form of the POMS,[13] which had been translated and validated for the Japanese general population.[14] While the POMS depicts sustained moods, previous studies have shown that it detects mood fluctuations within individuals.[16] Moreover, the test–retest reliability of POMS scores is not particularly high (0.65 to 0.74), suggesting that the score reflects a mood state rather than a personality trait.[15]

The participants rated 30 mood-related adjectives on a 5-point scale ranging from 0 ("not at all") to 4 ("extremely") on the basis of how they had been feeling during the past 1 week. The POMS consists of six identifiable mood factors: tension, depression, anger, vigor, fatigue, and confusion. In this study, we focused on the POMS depression score (POMS_D) because it had shown the most significant correlation with PFC activity for the verbal WM task in our previous study.[12]

2.3 *WM Tasks*

Immediately after the mood assessment, we measured the participants' PFC activity while they performed WM tasks. The tasks were presented through software (Platform of Stimuli and Tasks, developed at Hitachi's Central Research Laboratory), the same as in the previous study.[12] Each participant performed two types of WM tasks (verbal and spatial), which had an identical delayed-response paradigm. In both sessions, each task trial started with a 1500-ms presentation of the target stimuli (Target) on the PC display screen, which was followed by a delay of 7000 ms. A probe stimulus (Probe) was then presented for 2000 ms or until the participant responded. The participant responded by pressing a button on a handheld game controller connected to the PC. The system recorded the button pressed and the reaction time. In the verbal WM task, a set of two or four Japanese Hiragana characters were presented as the Target, and a Japanese Katakana character was presented as the Probe. The participants were instructed to judge whether the character presented as the Probe corresponded to any of the Target characters and then press the appropriate button. In the spatial WM task, the Target was the location of two or four white squares out of eight locations, and the Probe was the location of a white square. The participants were instructed to assess if the location of the white square presented as the Probe was identical to any of the locations of the squares presented as the Target. The intervals between the Probe onset and the following Target onset in the next trial were randomized from 16 to 24 s. Only a fixation cross was presented during the interval and delay period. In addition, a visual cue (changing the color of the fixation cross) was presented for 500 ms prior to trial onset. Auditory cues (1000- and 800-Hz pure tones of 100-ms duration) were presented at the onsets of the visual cue and Probe, respectively.

We organized the WM tasks into two sessions, one for the verbal WM task and the other for the spatial WM task, with a counterbalanced order across participants. Sixteen trials of one of the tasks were repeated in each session, and the sessions were separated by a short break (approximately 1 min). While in our previous experiment the WM task was intermingled with two additional conditions resulting in only five repetitions for each WM task, these conditions were not used in the present experiment. This modification made it possible to increase the number of repetitions for the WM task.

2.4 *OT Measurement*

The PFC activity was measured using an OT system (ETG-7100, Hitachi Medical Corporation, Japan). The system is based on a continuous wave (cw) NIRS technique.[9–11] Although other techniques such as time-resolved and frequency-domain techniques[17–19] are possibly advantageous for accurate estimation of brain tissue oxygenation and for depth-resolved analysis,[20–22] we used the cw NIRS technique because it has proved useful in previous practical studies.[23–28]

The OT system light sources were cw laser diodes with a wavelength of 695 or 830 nm. The average power of each source was 2 mW (for both wavelengths), and the two wavelength lights were irradiated on the skin through an incident optical fiber bundle (1.5-mm diameter). The signal intensities of the transmitted light were detected through a detection optical fiber bundle located 30 mm from the incident position at a sampling rate of 100 ms. We used 15 incident optical fiber bundles (sources) and 15 detection optical fiber bundles (detectors), which were arranged alternately, separated by 30 mm, in a 3×10 lattice pattern and embedded in a soft silicon holder. This resulted in a configuration with 47 measurement positions (defined as channels: chs), each corresponding to a midpoint of source-detector pair (Fig. 1). The holder was placed on each participant's forehead, and the optical fiber bundles contacted the skin on the forehead. Although we used a different system (ETG-4000, Hitachi Medical Corporation, Japan) in our previous study,[12] the basic specifications were common to both systems. The only difference between the two measurements was the width of the measurement area; the present study measured 47 chs (6×27 cm) using a 3×10 optode arrangement while our previous study measured 52 chs (6×30 cm) using a 3×11 optode arrangement.

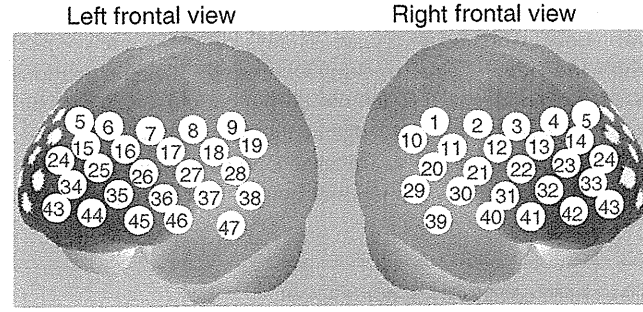

Fig. 1 Arrangement of measurement positions (47 channels) in MNI space, estimated using probabilistic registration method (Ref. 30).

The reduced width in the present study was due to a limitation in the system software. In addition, the primary activation areas identified in the previous study[12] were in the range of the measurement area of the present study.

To estimate the locations of the OT channels in the Montreal Neurological Institute (MNI) space, we used the probabilistic registration method.[29,30] Prior to the experiment, we corrected the sample data for the three-dimensional (3D) coordinates of the 30 optode locations and scalp landmarks (in accordance with the international 10 to 20 system: Fp1, Fp2, Fz, T3, T4, C3, C4) for the 11 participants. The data were recorded with a 3D-magnetic space digitizer (3D probe positioning unit for OT system, EZT-DM101, Hitachi Medical Corporation, Japan).

2.5 *Data Analysis*

Analysis was performed using the plug-in–based analysis software Platform for Optical Topography Analysis Tools (developed by Hitachi, CRL; run on MATLAB, The MathWorks, Inc., U.S.A.). First, the temporal data detected for the intensity change at each wavelength were used to calculate the products of the effective optical path length and the concentration changes of the independent hemoglobin (Hb) species ($\Delta C'_{\mathrm{oxy}}$: oxy-Hb signal, and $\Delta C'_{\mathrm{deoxy}}$: deoxy-Hb signal) for each channel on the basis of the modified Beer–Lambert law[31] as follows:

$$\Delta C'_{\mathrm{oxy}}=L\cdot\Delta C_{\mathrm{oxy}}=\frac{-\varepsilon_{\mathrm{deoxy}(\lambda 2)}\cdot\Delta A_{(\lambda 1)}+\varepsilon_{\mathrm{deoxy}}(\lambda 1)\cdot\Delta A_{(\lambda 2)}}{E}, \tag{1}$$

$$\Delta C'_{\mathrm{deoxy}}=L\cdot\Delta C_{\mathrm{deoxy}}=\frac{\varepsilon_{\mathrm{oxy}(\lambda 2)}\cdot\Delta A_{(\lambda 1)}-\varepsilon_{\mathrm{oxy}(\lambda 1)}\cdot\Delta A_{(\lambda 2)}}{E}, \tag{2}$$

where

$$E=\varepsilon_{\mathrm{deoxy}(\lambda 1)}\cdot\varepsilon_{\mathrm{oxy}(\lambda 2)}-\varepsilon_{\mathrm{deoxy}(\lambda 2)}\cdot\varepsilon_{\mathrm{oxy}(\lambda 1)}. \tag{3}$$

$\Delta C'_{\mathrm{oxy}}$ and $\Delta C'_{\mathrm{deoxy}}$ are expressed as the indefinite effective optical path length in the activation region (L) multiplied by the concentration change (ΔC_{oxy} and $\Delta C_{\mathrm{deoxy}}$). ΔA, $\varepsilon_{\mathrm{oxy}}$, and $\varepsilon_{\mathrm{deoxy}}$ indicate the logarithm of the intensity change in the detected light, the absorption coefficient of the oxygenated hemoglobin, and that of the deoxygenated hemoglobin, respectively, for the two wavelengths ($\lambda 1$, $\lambda 2$). We assume that the effective optical path length (L) is equal for every wavelength because accurate estimation of L is almost impossible with current techniques.[32] We used the oxy-Hb signals ($\Delta C'_{\mathrm{oxy}}$) in our analysis because we had previously observed clearer responses in these signals than in the deoxy-Hb signals.[12,33,34] To extract the task-related components from the raw oxy-Hb signals, we primarily used independent component analysis (ICA) following a published procedure.[35] Using this procedure, we reconstructed task-related oxy-Hb signals from the independent components that exceeded a criterion of 0.2 for the mean intertrial cross correlation.[35]

The time-continuous data of the oxy-Hb signals for each channel were separated into task blocks, which were defined as 25.5-s periods starting from 1.0 s before Target onset and ending 16.0 s after Probe onset, each containing a WM task trial. We removed blocks contaminated by a motion artifact, which was defined as a raw oxy-Hb signal change larger than 0.4 mM · mm over two successive samples (200-ms duration), as we did in our previous study.[12] We selected 0.4 mM · mm as the threshold level because we had found that sharp noises (putatively unphysiological signal changes) identified by a visual inspection of the data from our previous study[12] were effectively detected at this level. The remaining data were baseline corrected by linear regression based on the least squares method by using the data for the first second and the final second of each task block.

To evaluate PFC activity during the tasks, we defined the "activation period" as the 5-s period starting 5.0 s after Target onset, taking into consideration the delay in hemodynamic changes from neuronal activity mainly related to the encoding process. The mean signal changes during the activation period (x_i) were calculated for the oxy-Hb signal for each task block. Using the mean value of x_i across task blocks, we calculated within-participant z-values (converted from t-statistics) for each channel, taking intertrial variability into consideration as follows:

$$z=\frac{\overline{x}}{SD}, \tag{4}$$

where

$$\overline{x}=\frac{1}{n}\sum_{i=1}^{n}x_i, \tag{5}$$

and

$$SD=\sqrt{\frac{1}{n}\sum_{i=1}^{n}(x_i-\overline{x})^2}. \tag{6}$$

The z-values are expressed as the mean x_i [Eq. (5)] divided by the intertrial variability, which is given by the standard deviation of the x_i across task trials [Eq. (6)]. The z-values were defined as activation values (Act_V and Act_S) and represented the activation strengths for the verbal WM task (Act_V) and spatial WM task (Act_S). For the correlation analysis, we calculated the differences between successive sessions (Δ1st to 2nd and Δ2nd to 3rd) in Act_S (ΔAct_S), in Act_V (ΔAct_V), and in POMS_D (ΔPOMS_D) for each participant. These time-to-time fluctuations by individuals enabled us to identify the contribution of each participant's mood state on their PFC activity independent of trait factors. In the correlation analysis, the Spearman (rank) partial correlation with control variables of age and gender was used.

3 Results

Behavioral data (accuracy and reaction time: RT) for the WM tasks are listed in Table 1. An analysis of variance (ANOVA) with session order (1st, 2nd, and 3rd) and WM task (verbal and spatial) as within-participant factors revealed that there was no significant main effect of session order for both accuracy ($p = 0.47$) and RT ($p = 0.29$). On the other hand, a significant main effect of WM tasks was indicated for RT ($p = 0.005$), which means that RT for the verbal WM task was longer than that for the spatial WM tasks. However, the verbal WM task tended to show higher accuracy than the spatial WM task, though it was not significant ($p = 0.14$). The mean and standard deviation (SD) of POMS_D were 2.47 ± 2.67 for the 1st session, 1.88 ± 2.23 for the 2nd session, and 2.65 ± 2.91 for the 3rd session.

To examine the basic activation pattern during WM tasks, we first conducted across-participants t-test of the activation

Table 1 Mean accuracy and RT for WM tasks.

	Verbal			Spatial		
	1st	2nd	3rd	1st	2nd	3rd
Accuracy (%)	97.8	97.4	96.3	96.0	96.3	94.9
SD	4.8	5.1	7.2	7.4	7.2	9.3
RT (ms)	1250	1164	1165	1109	1122	1069
SD	208	188	263	205	261	255

values (Act_V and Act_S) for each session [Fig. 2(a)]. Channels in the bilateral dorsolateral PFC showed significantly positive values in all cases ($p < 0.05$). In particular, ch22 in the right hemisphere and ch26 in the left hemisphere consistently showed prominent activation ($p < 0.01$) for all sessions for both WM tasks [marked channels in Fig. 2(a)]. For these main activation channels, a session dependency (order effect) on the activation values was tested using the repeated-measures ANOVA with session order (1st, 2nd, and 3rd) and WM task (verbal and spatial). This analysis showed no main effect of the session order (ch22: $p = 0.96$, ch26: $p = 0.28$) with no interaction between session order and WM task (ch22: $p = 0.59$, ch26: $p = 0.76$), indicating the same activation pattern was reproduced for all sessions regardless of the WM type. The similarity of the time courses in activation signals among sessions is shown in Fig. 2(b). In addition, the main effect of WM tasks indicated no significant effect in the two channels (ch22: $p = 0.90$, ch26: $p = 0.15$).

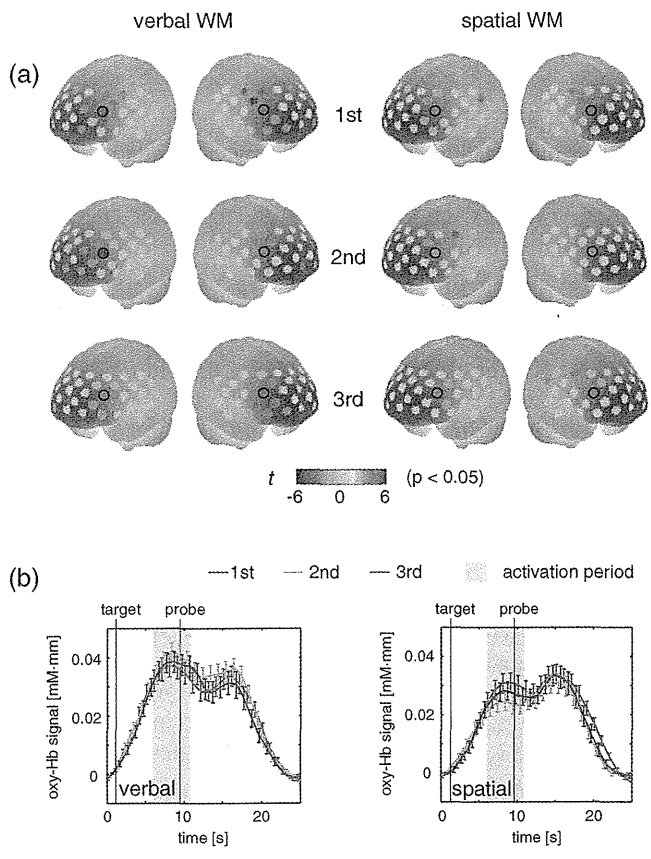

Fig. 2 Reproducibility of cortical activation for verbal and spatial WM tasks. (a) *t*-maps of activation values among participants. Channels with significant activation (determined with one-sample *t*-test against zero) are indicated with color scale shown below (two-tailed, $p < 0.05$). (b) Mean time courses of reconstructed oxy-Hb signals for representative channel (ch22 in Fig. 1). Yellow bars perpendicular to the *x*-axis indicate activation period (5-s duration). Error bars indicate standard errors across participants.

To reveal the relationship between within-individual changes in depressed mood state and PFC activation for WM tasks, we calculated the Spearman rank correlation coefficient (ρ) between ΔPOMS_D and ΔAct_V (or ΔAct_S) for each channel. The ρ-maps for Δ1st to 2nd and Δ2nd to 3rd are shown in Fig. 3(a). We regarded the channels, in which the *p*-values were less than 0.05 for both Δ1st to 2nd and Δ2nd to 3rd, as significantly correlated. This result indicated significantly negative correlations between ΔPOMS_D and ΔAct_V for channels mainly located in the left dorsolateral PFC (ch26 and ch35) and around the left pre-motor and supplementary motor cortex (ch8 and ch19). In contrast, the correlation coefficients between ΔAct_S and ΔPOMS_D did not reach statistical significance (the higher $p > 0.21$). These results were consistent with our previous results.[12] The distributions of ρ-values among[12] channels are shown with histograms [Fig. 3(b)] to demonstrate the discrepancy between ΔAct_V and ΔAct_S.

Figure 4 shows the negative correlation between ΔPOMS_D and ΔAct_V in the left dorsolateral PFC (ch26 and ch35), where clear WM-related activity was demonstrated (Fig. 2). The *p*-values for the correlation coefficients were 0.0315 and 0.0292 for Δ1st to 2nd and Δ2nd to 3rd, respectively. These *p*-values mean that the probability of obtaining these correlation coefficients is 0.00092 (0.0315×0.0292), which is below the corrected *p*-value of 0.05 for all 47 channels (0.05/47 = 0.00106). This indicates that decreased depressed mood score (POMS_D) is correlated with increased PFC activity for the verbal WM task (Act_V).

The within-individual fluctuations of POMS_D and Act_V (mean of ch26 and ch35) are shown in Fig. 5 for all participants, where the POMS_D is denoted on the reversed *Y*-axis. Although the sensitivities might be different, the basic change pattern for Act_V and reversed POMS_D across sessions appears to be similar in most participants.

4 Discussion

We used OT to show that fluctuations in the depressed mood state within individuals are correlated with their PFC activity during a verbal WM task. The results are consistent with those of our previous study[12] and confirm the state-dependent feature of PFC activity, which cannot be explained by the effects of certain trait differences among individuals.

The mean activation patterns for WM tasks were well reproduced, as shown in Fig. 2. The central channels of the activation were located in the dorsolateral PFC, which is consistent with other fMRI studies.[36] Moreover, the strong similarity between the activation patterns found in the present study with those found in our previous study[12] suggests that OT measurement is highly reliable for detecting cortical activity for these WM tasks. We found no main effect of session order for the PFC activity, suggesting that there was no simple order effect in our

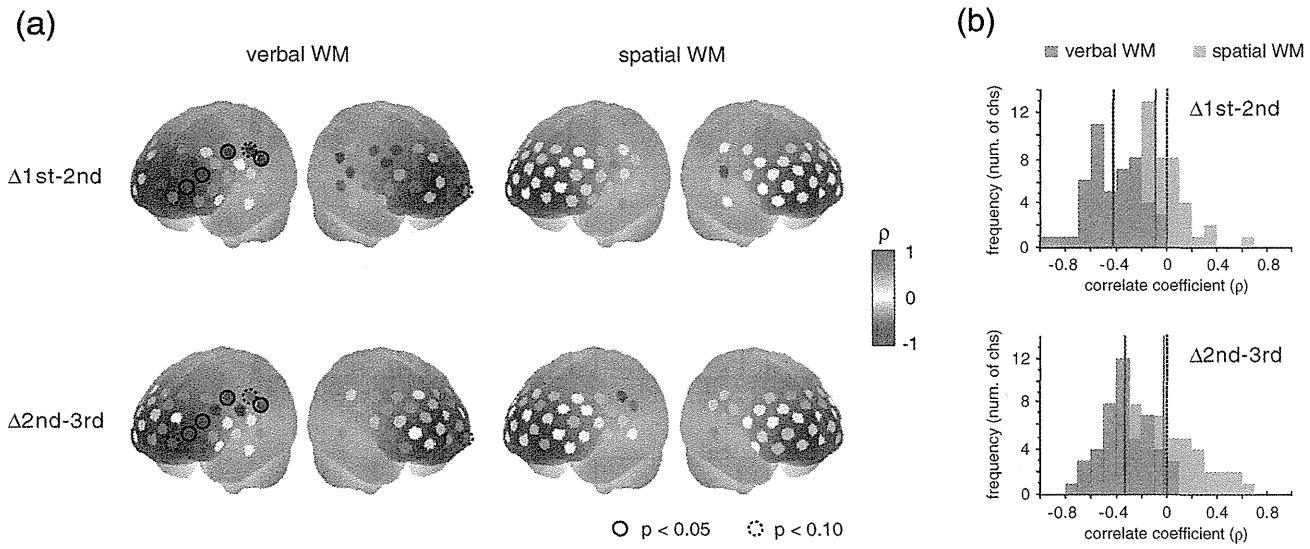

Fig. 3 Relationship between variations in depressed mood state (POMS_D) and those in activation values for verbal and spatial WM tasks (Act_V and _Act_S). (a) Statistical ρ-maps indicating correlation coefficients (Spearman ρ) between ΔPOMS_D and ΔAct_V (or ΔAct_S). Channels that showed correlation coefficients ($p < 0.05$) in both Δ1st to 2nd and Δ2nd to 3rd are marked with solid circles. In addition, channels that showed correlation coefficients ($p < 0.10$) in both Δ1st to 2nd and Δ2nd to 3rd are marked with dashed circles. (b) Histograms illustrating distributions of ρ-values for each WM task. Blue vertical line denotes median ρ-value for verbal WM task, and red vertical line denotes median ρ-value for spatial WM task among 47 channels.

measurements. In addition, the oxy-Hb signals in a representative channel demonstrated overlapped time courses among three sessions. These results support that relevant cortical activity for WM functions can be extracted using ICA.[35] Regarding differences between verbal and spatial WM tasks, the activation regions for the verbal WM task appeared to be larger than those for the spatial WM task. However, no significant main-effect of WM tasks was found in the channels that showed significant correlation coefficients between ΔPOMS_D and ΔAct_V (ch8: $p = 0.94$, ch19: $p = 0.12$, ch26: $p = 0.15$, ch35: $p = 0.07$). In addition, the behavioral data did not reveal significant differences between the two tasks in terms of difficulty. The RT for the verbal WM task was longer than that for the spatial WM tasks, which was possibly due to a difference in the task strategy, as participants showed higher accuracy for the verbal WM task than for the spatial WM task.

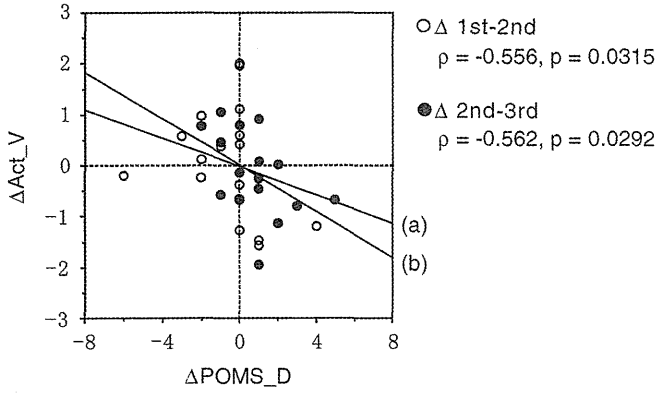

Fig. 4 Scatter plot showing relationship between ΔPOMS_D and ΔAct_V in left dorsolateral PFC (mean of ch26 and ch35). (a) Regression line of data for Δ1st to 2nd. (b) Regression line of data for Δ2nd to 3rd.

The basic activation patterns were thus similar in both WM tasks, but the correlation analysis revealed a contrast between tasks in relation to the depressed mood state (POMS_D). The negative correlation between ΔPOMS_D and ΔAct_V were well reproduced in the two independent differences between successive sessions (Δ1st to 2nd and Δ2nd to 3rd), while there were consistently no significant correlations between ΔPOMS_D and ΔAct_S. This result suggests that the PFC activity induced by a verbal WM task is selectively related to an individual's depressed mood state. In addition, the significant channels were mainly located in the left dorsolateral PFC, which is consistent with previous results.[12] Thus, we found that the interindividual variation in PFC activity during a verbal WM task[12] is not simply an indirect reflection of individual differences in trait factors; it actually reflects time-to-time fluctuations in the depressed mood state of an individual. Although the inherent limitation of transcranial NIRS requires that we consider the effect of hemodynamic changes in the extracerebral tissue, such as changes in skin blood flow,[37,38] our task paradigm did not impose intense physical or psychological demands, which could induce systemic changes. Moreover, the effect of extracerebral hemodynamic changes could not account for our finding that there is selective negative correlation between ΔPOMS_D and ΔAct_V in a localized area.

We plotted the within-individual fluctuations of POMS_D and Act_V (Fig. 5) to indicate the feasibility of using OT signals for assessing the depressed mood state of healthy participants. While Act_V apparently fluctuated in parallel with POMS_D within individuals, we could not estimate its effectiveness or validity because the depressed mood state is a psychological construct and difficult to define. To uncover new ways of using optical topography to obtain a potential state marker for an individual's mood state, we need to further clarify the interactions between the depressed mood state and PFC activity on the

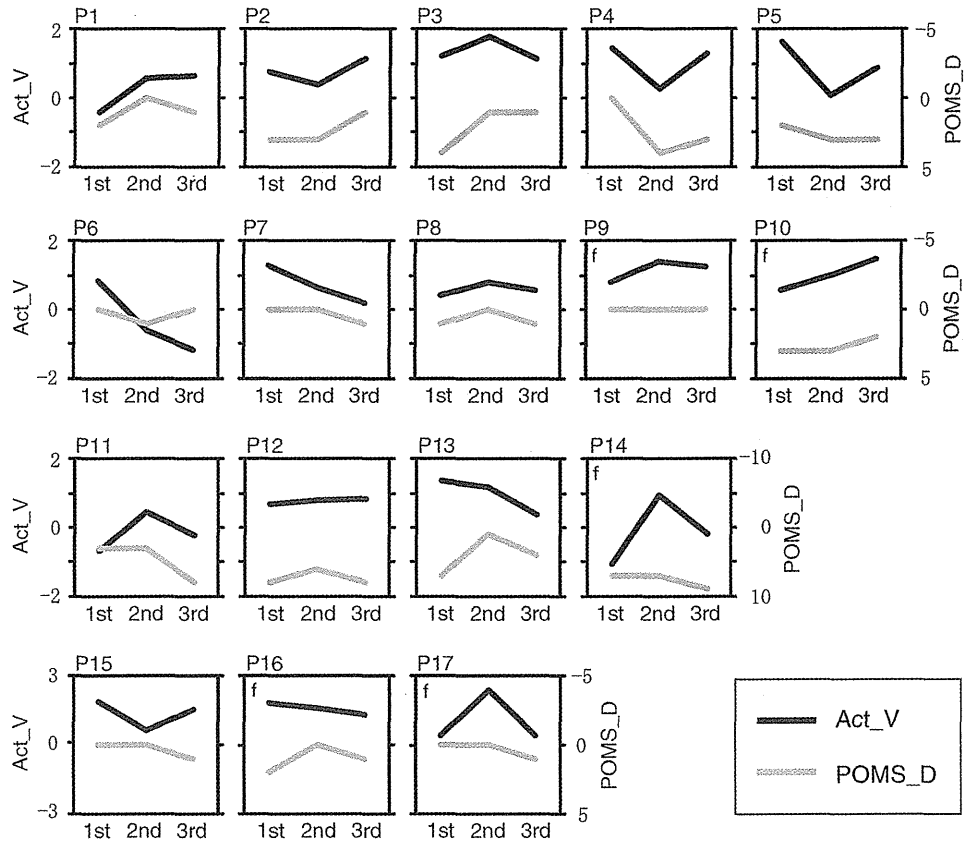

Fig. 5 Monthly fluctuations in POMS_D and Act_V (mean of ch26 and ch35) shown for every 2 weeks for all participants. Graphs with small "f" in top-left corner indicate data from females.

basis of neurophysiology, such as by using a pharmacological approach.[39–41]

5 Conclusion

We demonstrated that prefrontal cortex activity during a verbal working memory task varies depending on the participant's depressed mood state, independent of trait factors. This suggests that using optical topography to measure PFC activity during a verbal WM task can be used as a potential state marker for an individual's depressed mood state.

Acknowledgments

We thank Dr. Masashi Kiguchi, Dr. Atsushi Maki, and Dr. Kisou Kubota for their insightful comments and constructive suggestions during our discussions with them. We also thank Dr. Akiko N. Obata, Dr. Hirokazu Atsumori, Ms. Yukari Yamamoto, and Mr. Tsukasa Funane for their helpful support.

References

1. R. L. Mitchell and L. H. Phillips, "The psychological, neurochemical and functional neuroanatomical mediators of the effects of positive and negative mood on executive functions," *Neuropsychologia* **45**(4), 617–629 (2007).
2. L. Pessoa, "On the relationship between emotion and cognition," *Nat. Rev. Neurosci.* **9**(2), 148–158 (2008).
3. E. I. Bartolic, M. R. Basso, B. K. Schefft, T. Glauser, and M. Titanic-Schefft, "Effects of experimentally-induced emotional states on frontal lobe cognitive task performance," *Neuropsychologia* **37**(6), 677–683 (1999).
4. M. R. Basso, B. K. Schefft, M. D. Ris, and W. N. Dember, "Mood and global-local visual processing," *J. Int. Neuropsychol. Soc.* **2**(3), 249–255 (1996).
5. N. A. Harrison, L. Brydon, C. Walker, M. A. Gray, A. Steptoe, R. J. Dolan, and H. D. Critchley, "Neural origins of human sickness in interoceptive responses to inflammation," *Biol Psychiatry* **66**(5), 415–422 (2009).
6. S. Qin, E. J. Hermans, H. J. van Marle, J. Luo, and G. Fernandez, "Acute psychological stress reduces working memory-related activity in the dorsolateral prefrontal cortex," *Biol. Psychiatry* **66**(1), 25–32 (2009).
7. M. Suda, M. Fukuda, T. Sato, S. Iwata, M. Song, M. Kameyama, and M. Mikuni, "Subjective feeling of psychological fatigue is related to decreased reactivity in ventrolateral prefrontal cortex," *Brain Res.* **1252**, 152–160 (2009).
8. M. Suda, T. Sato, M. Kameyama, M. Ito, T. Suto, Y. Yamagishi, T. Uehara, M. Fukuda, and M. Mikuni, "Decreased cortical reactivity underlies subjective daytime light sleepiness in healthy subjects: a multichannel near-infrared spectroscopy study," *Neurosci. Res.* **60**(3), 319–326 (2008).
9. A. Maki, Y. Yamashita, Y. Ito, E. Watanabe, Y. Mayanagi, and H. Koizumi, "Spatial and temporal analysis of human motor activity using noninvasive NIR topography," *Med. Phys.* **22**(12), 1997–2005 (1995).
10. Y. Yamashita, A. Maki, Y. Ito, E. Watanabe, H. Mayanagi, and H. Koizumi, "Noninvasive near-infrared topography of human brain activity using intensity modulation spectroscopy," *Opt. Eng.* **35**, 1046–1099 (1996).
11. Y. Yamashita, A. Maki, and H. Koizumi, "Measurement system for noninvasive dynamic optical topography ," *J. Biomed. Opt.* **4**(4), 414–417 (1999).
12. R. Aoki, H. Sato, T. Katura, K. Utsugi, H. Koizumi, R. Matsuda, and A. Maki, "Relationship of negative mood with prefrontal cortex activity

during working memory tasks: An optical topography study," *Neurosci. Res.* **70**, 189–196 (2011).
13. P. M. McNair, M. Lorr, and L. F. Dropplemen, *Profile of Mood States Manual, Educational and Industrial Testing Service*, San Diego (1971).
14. K. Yokoyama, S. Araki, N. Kawakami, and T. Takeshita, "[Production of the Japanese edition of profile of mood states (POMS): assessment of reliability and validity]," *Nippon Koshu Eisei Zasshi* **37**(11), 913–918 (1990).
15. D. M. McNair and J. P. Heuchert, *Profile of Mood States Technical Update*, Multi-Health Systems, New York (2003).
16. B. G. Berger and R. W. Motl, "Exercise and mood: a selective review and synthesis of research employing the Profile of Mood States," *J. Appl. Sport Psychol.* **12**(1), 69–92 (2000).
17. A. Duncan, J. H. Meek, M. Clemence, C. E. Elwell, L. Tyszczuk, M. Cope, and D. T. Delpy, "Optical pathlength measurements on adult head, calf and forearm and the head of the newborn infant using phase resolved optical spectroscopy," *Phys. Med. Biol.* **40**(2), 295–304 (1995).
18. M. S. Patterson, B. Chance, and B. C. Wilson, "Time resolved reflectance and transmittance for the non-invasive measurement of tissue optical properties," *Appl. Opt.* **28**(12), 2331–2336 (1989).
19. M. S. Patterson, J. D. Moulton, B. C. Wilson, K. W. Berndt, and J. R. Lakowicz, "Frequency-domain reflectance for the determination of the scattering and absorption properties of tissue," *Appl. Opt.* **30**(31), 4474–4476 (1991).
20. D. Contini, A. Torricelli, A. Pifferi, L. Spinelli, F. Paglia, and R. Cubeddu, "Multi-channel time-resolved system for functional near infrared spectroscopy," *Opt. Express* **14**(12), 5418–5432 (2006).
21. M. Kacprzak, A. Liebert, P. Sawosz, N. Zolek, and R. Maniewski, "Time-resolved optical imager for assessment of cerebral oxygenation," *J. Biomed. Opt.* **12**(3), 034019 (2007).
22. H. Wabnitz, M. Moeller, A. Liebert, H. Obrig, J. Steinbrink, and R. Macdonald, "Time-resolved near-infrared spectroscopy and imaging of the adult human brain," *Adv. Exp. Med. Biol.* **662**, 143–148 (2010).
23. T. Grossmann, R. Oberecker, S. P. Koch, and A. D. Friederici, "The developmental origins of voice processing in the human brain," *Neuron* **65**(6), 852–858 (2010).
24. Y. Minagawa-Kawai, H. van der Lely, F. Ramus, Y. Sato, R. Mazuka, and E. Dupoux, "Optical brain imaging reveals general auditory and language-specific processing in early infant development," *Cereb. Cortex* **21**(2), 254–261 (2011).
25. M. Pena, A. Maki, D. Kovacic, G. Dehaene-Lambertz, H. Koizumi, F. Bouquet, and J. Mehler, "Sounds and silence: an optical topography study of language recognition at birth," *Proc. Natl. Acad. Sci. U.S.A.* **100**(20), 11702–11705 (2003).
26. H. Sato, T. Takeuchi, and K. L. Sakai, "Temporal cortex activation during speech recognition: an optical topography study," *Cognition* **73**(3), B55–B66 (1999).
27. S. Tsujimoto, T. Yamamoto, H. Kawaguchi, H. Koizumi, and T. Sawaguchi, "Prefrontal cortical activation associated with working memory in adults and preschool children: an event-related optical topography study," *Cereb. Cortex* **14**(7), 703–712 (2004).
28. E. Watanabe, A. Maki, F. Kawaguchi, K. Takashiro, Y. Yamashita, H. Koizumi, and Y. Mayanagi, "Non-invasive assessment of language dominance with near-infrared spectroscopic mapping," *Neurosci. Lett.* **256**(1), 49–52 (1998).
29. M. Okamoto and I. Dan, "Automated cortical projection of head-surface locations for transcranial functional brain mapping," *Neuroimage* **26**(1), 18–28 (2005).
30. A. K. Singh, M. Okamoto, H. Dan, V. Jurcak, and I. Dan, "Spatial registration of multichannel multi-subject fNIRS data to MNI space without MRI," *Neuroimage* **27**(4), 842–851 (2005).
31. D. T. Delpy, M. Cope, P. van der Zee, S. Arridge, S. Wray, and J. Wyatt, "Estimation of optical pathlength through tissue from direct time of flight measurement," *Phys. Med. Biol.* **33**(12), 1433–1442 (1988).
32. H. Sato, M. Kiguchi, F. Kawaguchi, and A. Maki, "Practicality of wavelength selection to improve signal-to-noise ratio in near-infrared spectroscopy," *Neuroimage* **21**(4), 1554–1562 (2004).
33. H. Sato, Y. Fuchino, M. Kiguchi, T. Katura, A. Maki, T. Yoro, and H. Koizumi, "Intersubject variability of near-infrared spectroscopy signals during sensorimotor cortex activation," *J. Biomed. Opt.* **10**, 044001 (2005).
34. H. Sato, M. Kiguchi, A. Maki, Y. Fuchino, A. Obata, T. Yoro, and H. Koizumi, "Within-subject reproducibility of near-infrared spectroscopy signals in sensorimotor activation after 6 months," *J. Biomed. Opt.* **11**(1), 014021 (2006).
35. T. Katura, H. Sato, Y. Fuchino, T. Yoshida, H. Atsumori, M. Kiguchi, A. Maki, M. Abe, and N. Tanaka, "Extracting task-related activation components from optical topography measurement using independent components analysis," *J. Biomed. Opt.* **13**(5), 054008 (2008).
36. E. E. Smith and J. Jonides, "Storage and executive processes in the frontal lobes," *Science* **283**(5408), 1657–1661 (1999).
37. S. Boden, H. Obrig, C. Kohncke, H. Benav, S. P. Koch, and J. Steinbrink, "The oxygenation response to functional stimulation: is there a physiological meaning to the lag between parameters?" *Neuroimage* **36**(1), 100–107 (2007).
38. T. Takahashi, Y. Takikawa, R. Kawagoe, S. Shibuya, T. Iwano, and S. Kitazawa, "Influence of skin blood flow on near-infrared spectroscopy signals measured on the forehead during a verbal fluency task," *Neuroimage* **57**(3), 991–1002 (2011).
39. F. G. Ashby, A. M. Isen, and A. U. Turken, "A neuropsychological theory of positive affect and its influence on cognition," *Psychol. Rev.* **106**(3), 529–550 (1999).
40. D. M. Barch, "Pharmacological manipulation of human working memory," *Psychopharmacology (Berlin)* **174**(1), 126–135 (2004).
41. M. Luciana, P. F. Collins, and R. A. Depue, "Opposing roles for dopamine and serotonin in the modulation of human spatial working memory functions," *Cereb. Cortex* **8**(3), 218–226 (1998).

Mol Cell Biochem
DOI 10.1007/s11010-011-0977-0

Pharmacological inhibition of HSP90 activity negatively modulates myogenic differentiation and cell survival in C2C12 cells

Akira Wagatsuma · Masataka Shiozuka · Naoki Kotake · Kawachi Takayuki · Honda Yusuke · Kunihiko Mabuchi · Ryoichi Matsuda · Shigeru Yamada

Received: 3 April 2011 / Accepted: 29 June 2011

Abstract Heat-shock protein90 (HSP90) plays an essential role in maintaining stability and activity of its clients. HSP90 is involved in cell differentiation and survival in a variety of cell types. To elucidate the possible role of HSP90 in myogenic differentiation and cell survival, we examined the time course of changes in the expression of myogenic regulatory factors, intracellular signaling molecules, and anti-/pro-apoptotic factors when C2C12 cells were cultured in differentiation condition in the presence of a HSP90-specific inhibitor, geldanamycin. Furthermore, we examined the effects of geldanamycin on muscle regeneration in vivo. Our results showed that geldanamycin inhibited myogenic differentiation with decreased expression of MyoD, myogenin and reduced phosphorylation levels of Akt1. Geldanamycin had little effect on the phosphorylation levels of p38MAPK and ERK1/2 but reduced the phosphorylation levels of JNK. Along with myogenic differentiation, geldanamycin increased apoptotic nuclei with decreased expression of Bcl-2. The skeletal muscles forced to regenerate in the presence of geldanamycin were of poor repair with small regenerating myofibers and increased connective tissues. Together, our findings suggest that HSP90 may modulate myogenic differentiation and may be involved in cell survival.

Keywords Apoptosis · HSP90 · JNK · Myogenic differentiation · Survival

Introduction

Heat-shock proteins (HSPs) are highly conserved set of cellular proteins that are quickly induced by stressful stimuli [1] to assist in the maintenance of cellular integrity and viability [2]. Under physiological conditions, HSP90 dynamically interacts with a diverse but highly select set of inherently unstable client proteins, including steroid hormone receptors, kinases, and transcription factors [3]. The HSP90 protein acts as molecular chaperone that regulates the cellular stress response by maintaining the conformation, stability, and function of client proteins [4].

Several lines of evidence suggest important roles for HSP90 in muscle physiology, such as myofibril assembly [5], somite development [6], muscle fiber lineages [7], and myogenic differentiation [8]. Yun et al. has been, for the first time, reported that myotube formation is blocked when C2C12 cells are treated with HSP90-specific inhibitor, geldanamycin [8]. However, since their study is based on qualitative data, it is arguable to what extent pharmacological inhibition of HSP90 activity suppresses myogenic differentiation. Geldanamycin specifically interferes with this association by occupying the ATP-binding pocket of HSP90 and dissociates client proteins from the chaperone, which results in their degradation by the ubiquitin-dependent

A. Wagatsuma (✉) · M. Shiozuka · K. Takayuki · H. Yusuke · R. Matsuda
Graduate School of Arts and Sciences, The University of Tokyo, Tokyo, Japan
e-mail: wagatsuma1969@yahoo.co.jp

A. Wagatsuma · K. Mabuchi
Graduate School of Information Science and Technology, The University of Tokyo, Tokyo, Japan

N. Kotake
Department of Fisheries Distribution and Management, National Fisheries University, Yamaguchi, Japan

S. Yamada
Department of Food and Health Sciences, Jissen Women's University, Tokyo, Japan

Published online: 08 July 2011

proteasome pathway [9]. Geldanamycin causes depletion of ErbB2, Akt, and Fyn, protein kinases [8] whose functions are required for myogenic differentiation [10] and for the survival of myoblasts and myofibers [11–13]. Geldanamycin also appears to attenuate mitogen-activated protein kinase (MAPK) signaling pathways, which control key cellular functions, including proliferation, differentiation, and survival [14]. Three distinct subgroups of MAPK pathways can be distinguished in mammalian cells: p38 mitogen-activated protein kinases (p38MAPK), extracellular signal-regulated kinase 1/2 (ERK1/2), c-Jun NH(2)-terminal kinase 1/2/3 (JNK1/2/3). Destabilization of Raf-1 by geldanamycin leads to disruption of the Raf-1–MEK–ERK1/2 signaling pathway in NIH 3T3 cells [15]. Geldanamycin abolishes TNFα-mediated activation of JNK in MCF-7 cells [16] and inhibits activation of p38MAPK in NRK-52E cells [17]. Even though MAPK signaling pathways are involved in myogenic differentiation [18–20], it remains to be elucidated whether geldanamycin-mediated inhibition of HSP90 activity has an impact on MAPK pathways in myogenic cells.

Geldanamycin has shown to induce apoptotic cell death in a variety of cell types. For example, when incubating with geldanamycin, apoptotic cell death is induced in PC12 cells [21]. Geldanamycin causes dissociation of HSP90-Bcl-2, initiating the release of cytochrome *c* from mitochondria and subsequently increasing the activity of caspases, resulting apoptosis in mast cells [22]. Although it has been reported that apoptotic cell death occurs in geldanamycin-treated myogenic cells [8], there are not yet sufficient data to elucidate the effect of geldanamycin on the occurrence of apoptosis of myogenic cells.

Here, we report that pharmacological inhibition of HSP90 activity using geldanamycin suppresses myogenic differentiation with decreased expression of MyoD and myogenin and reduced phosphorylation levels of Akt1 and JNK. Along with myogenic differentiation, geldanamycin causes apoptosis with decreased expression of Bcl-2. Our results suggest that HSP90 may be necessary for regulating myogenic differentiation and cell survival through its ability to control the multiple HSP90-dependent signaling pathways.

Materials & methods

Culture of mouse myogenic cell line

C2C12 myogenic cells [23] were maintained in growth medium comprising Dulbecco's minimum essential medium (DMEM) (GIBCO BRL, LifeTechnologies Inc., Grand Island, NY) containing 20% fetal bovine serum (FBS) (Equitec-Bio, Inc., Kerrville, TX), 4 mM L-glutamine, 100 U/ml penicillin, and 100 μg/ml streptomycin (Sigma-Aldrich, Inc. St. Louis, MO) at 37°C in 5% CO_2 and 95% air. Cells were seeded on a tissue culture dish in growth medium, and 24 h later, the medium was replaced with differentiation medium consisting of DMEM supplemented with 5% horse serum (HyClone Laboratories, Inc., Logan, UT). The cells approached 70-80% confluency in growth medium (day 0) and maintained in differentiation medium (24-96 h). The cells cultured in differentiation medium were treated with dimethylsulfoxide (DMSO) or 20 nM geldanamycin (Enzo Life Sciences International, Inc., Plymouth Meeting, PA) for 24–96 h as indicated in the legend to the figures. The medium was changed every 24 h. Geldanamycin derivative, 17-(Allylamino)-17-desmethoxygeldanamycin (17-AAG) (Enzo Life Sciences Inc., Faimingdale, NY) was also used as indicated in the legend to the figures.

Animal care

Male 4-week-old C57BL/6 J (B6) mice were used and were housed in the animal facility under a 12-h light/12-h dark cycle at room temperature (23 ± 2°C) and 55 ± 5% humidity. The mice were maintained on a diet of CE-2 rodent chow (Clea Japan, Meguro, Tokyo) and given water *ad libitum*. The mice were procured after approval for the present study from The University of Tokyo Animal Ethics Committee.

Induction of muscle degeneration/regeneration

Muscle degeneration/regeneration was induced as previously described [24]. Glycerol (100 μl of 50% vol/vol) was injected in three injection sites of gastrocnemius muscle. This model provokes hypercontraction of myofibers, degeneration, and necrosis of myofibers within 24 h after the injection and shows subsequent regeneration of myofibers between 7 and 14 days after the injection. The gastrocnemius muscles were isolated at various time points after muscle injury. To inhibit the activity of HSP90, 50 μl of treatment (178 μM) or DMSO was introduced into the muscle surrounding the injury site by direct intramuscular injection at day 1, 3, 5, and 7 after the initial injury. The gastrocnemius muscles were isolated at day 10 for histochemical analysis. All procedures in the animal experiments were performed in accordance with the guidelines presented in the Guiding Principles for the Care and Use of Animals in the Field of Physiological Sciences, published by the Physiological Society of Japan.

Creatine phosphokinase (CPK) activity assay

Cells were cultured as described above. Cells were washed twice with phosphate-buffered saline (PBS) and then

scraped from the surface of dish in the presence of PBS. The cell suspension was homogenized for 1 min. Lysates were centrifuged for 10 min at 13,000× *g*, the supernatants were collected, and the protein content in the samples was measured using a microbicinchoninic acid (BCA) assay (Pierce Chemical Co., Rockford, IL). CPK activity was measured with an automated analyzer, DRI-CHEM 3500 (Fuji Film Inc., Ashigara, Kanagawa). We calculated the activity of CPK (units per milligram of protein) after correction of total protein.

Immunoblot analysis

Total cellular protein extracts were prepared from whole gastrocnemius muscle or by rinsing cultures with PBS, then scraping the cells directly into sample buffer [25]. Protein concentration was determined by BCA assay. Protein was analyzed by sodium dodecyl sulfate–polyacrylamide gel electrophoresis (SDS–PAGE) and transferred to polyvinylidene fluoride membranes (Millipore Corp., Bedford, MA). Membranes were blocked with Odyssey Blocking Buffer (LI-COR Biosciences, Inc., Lincoln, NE) and incubated for 1 h with rabbit polyclonal anti-HIF-1α antibody (ZMD.417; Zymed Laboratories, Inc., South San Francisco, CA), anti-HSP90 antibody (SPC-104; Stressmarq Biosciences Inc., Victria, BC), anti-myogenin antibody (M225; Santa Cruz Biotechnology, Inc., Santa Cruz, CA), anti-β tubulin antibody (ab6046; Abcam Inc., Cambridge, MA), rabbit monoclonal anti-pan-Akt1 antibody (clone Y89; Epitomics Inc., Burlingame, CA), anti-phospho-Akt1^{Ser473} antibody (clone EP2109Y; Epitomics), anti-Bcl-2 antibody (clone E17; Epitomics), anti-Bax antibody (clone E63; Epitomics), anti-glyceraldehyde-3-phosphate dehydrogenase (GAPDH) antibody (clone EPR1977Y; Epitomics), mouse monoclonal anti-MyoD antibody (clone 5.8A; DakoCytomation Inc., Carpinteria, CA), anti-sarcomeric myosin heavy chain (sMyHC) antibody [clone MF20; Developmental Studies Hybridoma Bank (DSHB), Iowa City, IA], anti-pan-p38α/SAPK2α antibody (612168; BD Transduction Laboratories), anti-phospho-p38MAPK$^{Thr180/Tyr182}$ antibody (612280; BD Transduction Laboratories), anti-ERK1 antibody (610030; BD Transduction Laboratories, Lexington, KY), anti-phospho-ERK1/2$^{Thr202/Tyr204}$ antibody (612358; BD Transduction Laboratories), anti-pan-JNK/SAPK1 antibody (610627; BD Transduction Laboratories), and anti-phospho-JNK$^{Thr183/Tyr185}$ antibody (612540; BD Transduction Laboratories). Membranes were washed and incubated with goat anti-rabbit IgG antibody conjugated with Alexa Fluor 680 (Molecular Probes Inc., Eugene, OR) and rabbit anti-mouse IgG antibody conjugated with IRDye800 (Rockland Immunochemicals Inc., Gilbertsville, PA) and analyzed with an Odyssey Infrared Imaging System (LI-COR). Gel densitometries were quantified by using ImageJ software (Ver. 1.42, http://rsb.info.nih.gov/ij/). To verify equal loading, membranes were probed with anti-β-tubulin antibody or stained with IRDye Blue Protein Stain (LI-COR).

Immnocytochemical analysis

Cells were fixed with 3.8% paraformaldehyde, permeabilized with 0.5% TritonX-100, and then incubated with a mouse monoclonal anti-sarcomeric myosin heavy chain (sMyHC) (DSHB). After washes in PBS, primary antibody binding was visualized with goat anti-rabbit IgG antibody conjugated with goat anti-mouse IgG antibody conjugated with Alexa Fluor 594 (Molecular Probes) for 30 min before washing and mounting in fluorescent mounting medium (DakoCytomation) containing Hoechst 33258. The fusion index is defined as the percentage of nuclei present in myotubes (>2 nuclei) compared with the total number of nuclei present in the observed field. The diameter of myotubes was measured using ImageJ software (National Institutes of Health, Bethesda, MD; available at http://rsb.info.nih.gov/ij/). The average diameter *per* myotube was calculated as the mean of five measurements taken along the length of the myotube. The length of myotube was measured.

Identification of apoptotic nuclei

To confirm the presence of DNA cleavage, which characteristically occurs in apoptotic cells, we identified apoptotic nuclei in the presence or absence of geldanamycin. Apoptotic nuclei were detected by a terminal deoxynucleotidyl transferase (TdT) dUTP nick-end labeling (TUNEL) method using In situ Apoptosis Detection Kit (TaKaRa Bio, Inc., Otsu, Shiga). The cells were fixed in 4% paraformaldehyde, permeabilized with 0.1% Triton X-100 in 0.1% sodium citrate, and incubated with TdT and fluorescein-dUTP at 37°C for 60 min. Nuclei were counterstained with propidium iodide (Sigma-Aldrich). Apoptotic nuclei frequency was evaluated as the percentage of cells/1000 nuclei.

Histochemical analysis

The tissues were transversely sectioned at 8 μm using a cryostat at −20°C and thawed on 3-amino propylethoxysilane-coated slides. The sections were fixed with 4% paraformaldehyde for 10 min. The sections were washed with PBS, blocked with PBS containing 5% bovine serum albumin and 0.1% Igepal (Sigma-Aldrich, Inc. St. Louis, MO), and then incubated overnight at 4°C with a rabbit polyclonal anti-HSP90 antibody (Stressmarq Biosciences). The sections were incubated with goat anti-rabbit IgG antibody conjugated with goat anti-rabbit IgG antibody conjugated with Alexa Fluor 594 (Molecular Probes) for

30 min at room temperature. The sections were stained with Hoechst 33258 (Sigma-Aldrich). For negative control, the sections were processed in the same way, except that the primary antibody was omitted (Data not shown). The sections were stained with hematoxylin and eosin for evaluation of general muscle architecture. For morphometrical analysis, randomly selected fields were photographed (original magnification, X100; six fields per sample). Areas occupied by myofibers or non-myofibers and fiber cross-sectional area were determined using ImageJ software.

Statistical analysis

Data are means ± standard deviation (SD). Unpaired Student's *t*-test was used to determine significance. The level of significance was set at $P < 0.05$.

Result

Effects of geldanamycin on the expression levels of HSP90 client protein, HIF-1α, in differentiating C2C12 cells

The benzoquinone ansamycin antibiotics, geldanamycin, are characterized by its ability to specifically bind to and disrupt the function of the chaperone protein HSP90, leading to the depletion of multiple oncogenic client proteins. Since HIF-1α has shown to be a HSP90 client protein [26], we examined the effects of geldanamycin on the expression levels of HIF-1α in differentiating C2C12 cells. Upon reaching confluence, C2C12 cells were cultured in differentiation medium with 20 nM geldanamycin or its vehicle solvent DMSO for 24 h or 96 h, and then total cellular extract was prepared for HIF-1α expression levels by immunoblot analysis. The amount of HIF-1α in differentiating C2C12 cells treated with geldanamycin was decreased compared with that in differentiating C2C12 cells treated with DMSO after 24 h and 96 h (Fig. 1).

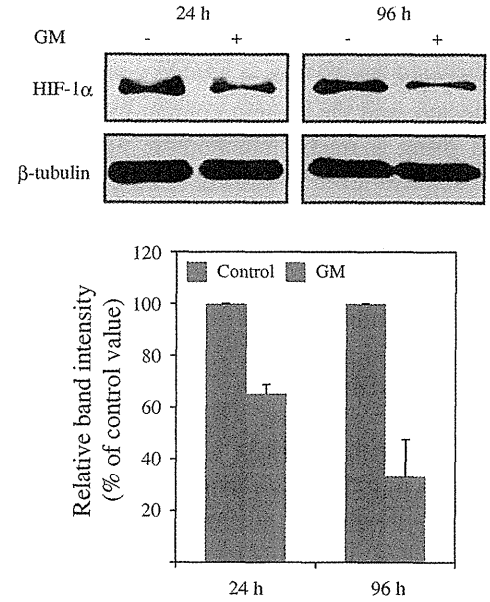

Fig. 1 Effects of geldanamycin treatment on expression levels of HSP90 client protein, HIF-1α, in differentiating C2C12 cells. Confluent cells were cultured in differentiation medium with DMSO or geldanamycin (GM) for 24 h or 96 h. The expression levels of HIF-1α were determined by immunoblot analysis with anti-HIF-1α antibody. Histograms represent the changes in the expression levels of HIF-1α. β-Tubulin was used as a loading control. The intensities of bands were measured and normalized to the control (DMSO) values. The data are the means ± SD ($n = 3$)

Pharmacological inhibition of HSP90 activity suppresses myogenic differentiation

Mouse C2C12 myoblasts have been widely used as an in vitro model to investigate the regulatory mechanisms underlying myogenic differentiation [27]. Myogenic differentiation is associated with a large increase in protein synthesis of muscle-specific proteins and enzymes involved in muscle contractions [28, 29]. To examine the effect of pharmacological inhibition of HSP90 activity on the amount of total cellular proteins during myogenic differentiation, we measured the amount of total cellular protein extracted from the C2C12 cells cultured in the presence or absence of geldanamycin. In contrast to untreated C2C12 cells, an increase in the amount of protein associated with myogenic differentiation was severely suppressed in the treated C2C12 cells (Fig. 2a). The amount of protein in the treated C2C12 cells was less than half of that in the untreated C2C12 cells 96 h after the initiation of myogenic differentiation. To quantify differentiation, the rate of muscle CPK activity was measured as a parameter of terminal myogenic differentiation. The CPK activities in the treated C2C12 cells were significantly lower than that in the untreated C2C12 cells 96 h after the initiation of myogenic differentiation (Fig. 2b). We also examined the effects of geldanamycin on the expression of sMyHC, another terminal differentiation marker. In the untreated C2C12 cells, the expression levels of sMyHC increased to a peak 96 h after the initiation of myogenic differentiation, whereas in the treated C2C12 cells, that of sMyHC was observed at 72 h but severely suppressed (Fig. 2c). To further characterize the inhibitory effect of geldanamycin on myogenic differentiation, we immunohistochemically examined expression of sMyHC in C2C12 cells cultured in differentiation medium after 96 h. As expected, the treatment of geldanamycin dramatically blocked myotube formation. The myotubes cultured in the presence of geldanamycin were shorter and thinner than

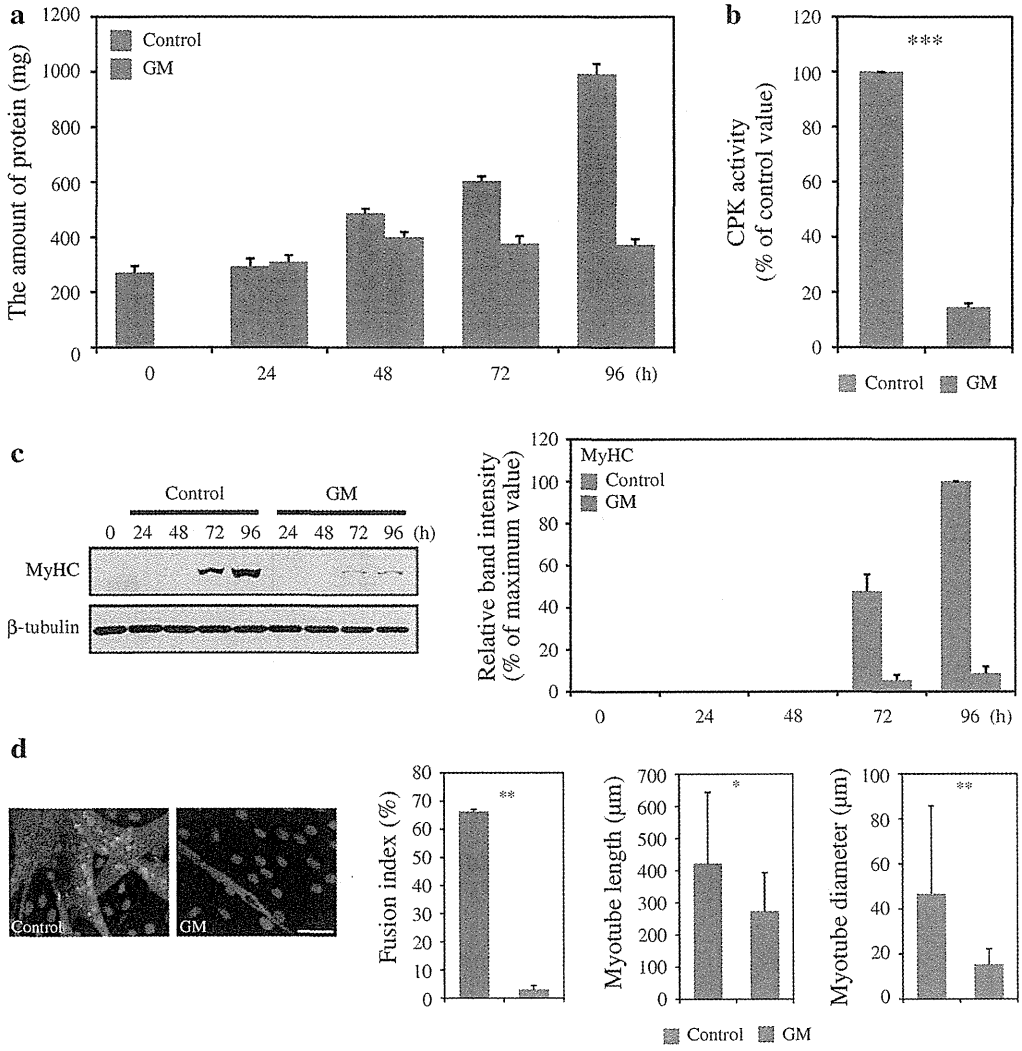

Fig. 2 Effects of geldanamycin treatment on the amount of total protein, CPK activity, and on expression levels of sMyHC protein during myogenic differentiation. Cells maintained in differentiation medium were treated with DMSO or geldanamycin for the time indicated in the figure (24-96 h). **a** Cells were harvested at 0, 24, 48, 72, or 96 h, and protein concentration was determined by BCA assay. Histogram represents the temporal changes in the amount of total protein during myogenic differentiation (n = 3/time point). **b** The CPK activity was measured with an automated analyzer at 96 h after induction of myogenic differentiation. Histogram represents relative changes in CPK activity. The data are expressed as a percentage change relative to control value arbitrary set to 100%. The data are the means ± SD of at least six independent experiments. **c** The level of sMyHC was determined by immunoblot analysis with anti-sMyHC antibody. Histogram represents the temporal changes in expression of sMyHC protein during myogenic differentiation (n = 3/time point). β-Tubulin was used as a loading control. The intensities of bands were measured and normalized to the maximum value observed during 4 days in culture. **d** For immunocytochemical analysis, the cells were cultured for 96 h and then fixed with paraformaldehyde. The cells were stained with anti-sMyHC, and nuclei were counterstained with Hoechst 33258. *Scale bar* = 100 μm. Histogram represents fusion index (nuclei inside myotubes/total number of nuclei), myotube length, or diameter (n = 6). The myotube length and diameter were measured with the image analysis system, calibrated to transform the number of pixels (viewed on a computer monitor) into micrometers. The data are the means ± SD of at least six independent experiments. These were statistically significant differences compared to the control (Ct): $^*P < 0.05$, $^{**}P < 0.01$, $^{***}P < 0.001$

those in the absence of geldanamycin. The fusion index for the C2C12 cells cultured in the absence of geldanamycin was 66.3 ± 0.8%, whereas the fusion index for the C2C12 cells cultured in the presence of geldanamycin was 3.0 ± 1.5%. The myotube length and diameter were significantly decreased in geldanamycin-treated cells compared with control cells (Fig. 2d).

Pharmacological inhibition of HSP90 activity decreases the expression levels of myogenic regulatory factors MyoD and myogenin upon induction of myogenic differentiation

Myogenesis is orchestrated through a series of transcriptional controls governed by the myogenic regulatory

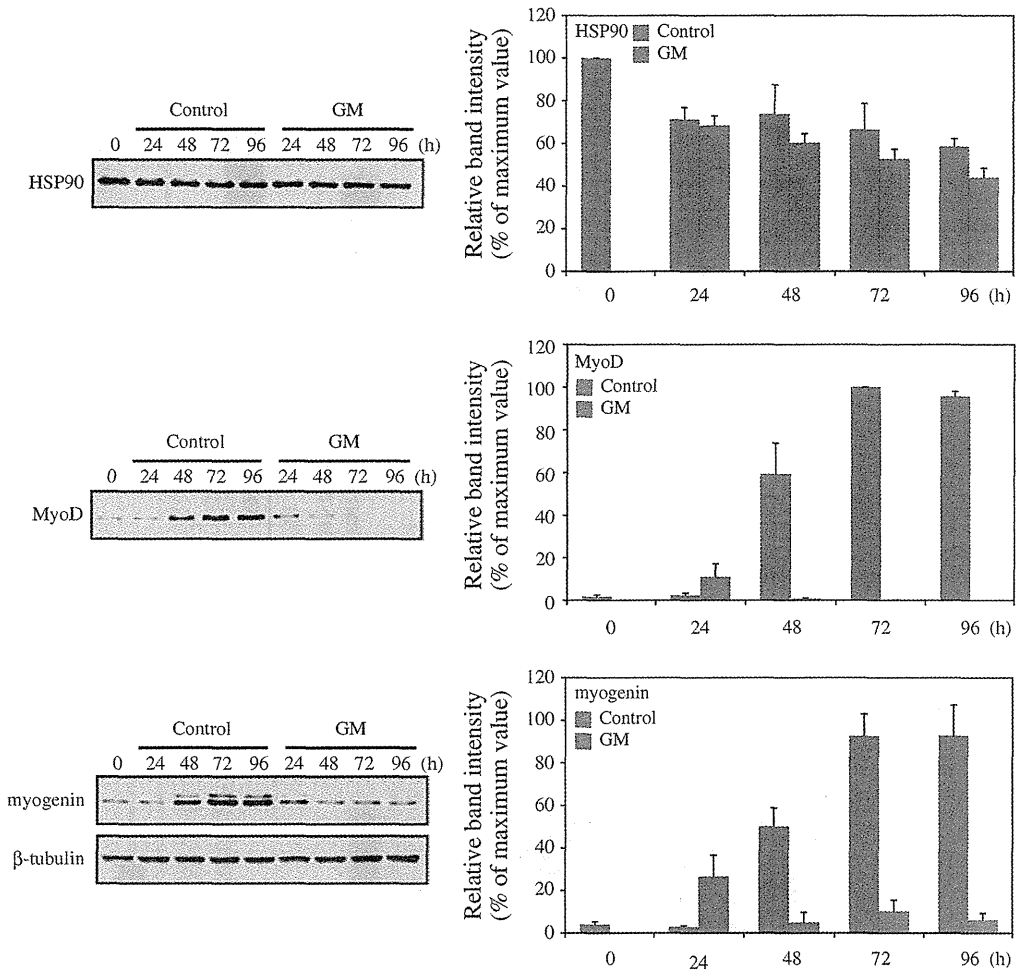

Fig. 3 Effects of geldanamycin treatment on expression of HSP90, MyoD, and myogenin proteins during myogenic differentiation. The expression levels of each protein were determined by immunoblot analysis with anti-HSP90, anti-MyoD, anti-myogenin, or anti-β-tubulin antibodies. Histograms represent the temporal changes in expression of each protein during myogenic differentiation. β-Tubulin was used as a loading control. The intensities of bands were measured and normalized to the maximum value observed during 4 days in culture. The data are the means $\pm$ SD ($n = 3$/time point)

factors. It has been well established that activated satellite cells are characterized by expression of MyoD and Myf5, whereas myoblast terminal differentiation is characterized by expression of myogenin and MRF4 [30]. We examined the effect of geldanamycin on the expression levels of MyoD and myogenin as well as HSP90 proteins during myogenic differentiation (Fig. 3). The expression levels of MyoD and myogenin proteins were gradually increased after initiation of myogenic differentiation and peaked at 72 h. The treatment of geldanamycin transiently increased the expression levels of MyoD and myogenin proteins at 24 h and then reduced the levels of these proteins during myogenic differentiation. The expression levels of HSP90 protein were slightly decreased during myogenic differentiation irrespective of geldanamycin treatment.

Pharmacological inhibition of HSP90 activity reduces phosphorylation of JNK during myogenic differentiation

Given that the extracellular signals that regulate the myogenic program are transduced to the nucleus by MAPKs [19], we examined the effect of geldanamycin on the phosphorylation levels of p38MAPK$^{Thr180/Tyr182}$, ERK1/2$^{Thr202/Tyr204}$, and JNK$^{Thr183/Tyr185}$ during myogenic differentiation (Fig. 4). As shown in Fig. 4, there were no significant differences in the phosphorylation levels of p38MAPK$^{Thr180/Tyr182}$ and ERK1/2$^{Thr202/Tyr204}$ proteins between control and geldanamycin treatment. The phosphorylation levels of JNK$^{Thr183/Tyr185}$ protein were decreased when the cells were cultured in the presence of geldanamycin. There were no significant differences in the expression levels of p38MAPK, ERK1/2, and JNK proteins between control and geldanamycin treatment.

Pharmacological inhibition of HSP90 activity reduces abundance and phosphorylation of Akt1 during myogenic differentiation

The serine/threonine kinase Akt, also known as protein kinase B (PKB), can substitute for phosphatidylinositol-3-kinase (PI3K) in the stimulation of myogenesis, and it may be an essential downstream component of PI3K-induced myogenic differentiation [10]. During myogenic differentiation, Akt